75N29118
19750021045

NASA TECHNICAL MEMORANDUM

NASA TM X-3262 c.1

NASA TM X-3262

EVALUATION BY STEP RESPONSE TESTS OF PROTOTYPE RELIEF VALVES DESIGNED FOR YF-12 INLET STABILITY BLEED SYSTEM

Miles O. Dustin and George H. Neiner

Lewis Research Center
Cleveland, Ohio 44135

NATIONAL AERONAUTICS AND SPACE ADMINISTRATION • WASHINGTON, D. C. • AUGUST 1975

1. Report No. NASA TM X-3262	2. Government Accession No.	3. Recipient's Catalog No.
4. Title and Subtitle EVALUATION BY STEP RESPONSE TESTS OF PROTOTYPE RELIEF VALVES DESIGNED FOR YF-12 INLET STABILITY BLEED SYSTEM		5. Report Date August 1975
		6. Performing Organization Code
7. Author(s) Miles O. Dustin and George H. Neiner		8. Performing Organization Report No. E-8135
		10. Work Unit No. 743-03
9. Performing Organization Name and Address Lewis Research Center National Aeronautics and Space Administration Cleveland, Ohio 44135		11. Contract or Grant No.
		13. Type of Report and Period Covered Technical Memorandum
12. Sponsoring Agency Name and Address National Aeronautics and Space Administration Washington, D. C. 20546		14. Sponsoring Agency Code
15. Supplementary Notes		

16. Abstract

Two stability bleed system relief valves were tested in a special dynamic test facility. These poppet valves are prototypes for a stability bleed system designed for use in a YF-12 flight inlet. One valve is unshielded, while the other has a special shield to eliminate the flow effect pressures on the piston. The tests determined the size of a damping orifice to be used during wind tunnel tests of the bleed system and verified an analog simulation of the valves. The effects of initial pressure level, pressure step size, and spring rate were investigated.

17. Key Words (Suggested by Author(s)) Supersonic inlets; Air intakes; Shock stability; Stability bypass; Jet engine inlets; Inlet bleed		18. Distribution Statement Unclassified - unlimited STAR Category 07 (rev.)	
19. Security Classif. (of this report) Unclassified	20. Security Classif. (of this page) Unclassified	21. No. of Pages 45	22. Price* $3.75

* For sale by the National Technical Information Service, Springfield, Virginia 22161

EVALUATION BY STEP RESPONSE TESTS OF PROTOTYPE RELIEF VALVES DESIGNED FOR YF-12 INLET STABILITY BLEED SYSTEM

by Miles O. Dustin and George H. Neiner

Lewis Research Center

SUMMARY

Two stability bleed system relief valves were built for dynamic performance evaluation. The valves are prototypes of valves designed for use in a stability bleed system to be incorporated into a YF-12 flight inlet for wind tunnel evaluation. The valves were tested in a special dynamic valve test facility. An important purpose of the test was to determine the size of a damping orifice to be used in the valves during wind tunnel tests of a stability bleed system installed in the YF-12 inlet. The effects of initial pressure level, size of pressure step, and spring rate were studied for three orifice sizes. The results of the transient tests were also used to verify the accuracy of an analog computer simulation of the valve. This was done so that the simulation could be used to predict valve performance under various wind tunnel and flight conditions.

One valve is a direct-acting poppet relief valve. In the stability bleed system the valve vents air overboard from a porous bleed region on the cowl inside surface just upstream of the throat. This valve has an underdamped response and will require a small orifice for damping.

The other valve tested is similar but has a shield that isolates the bottom of the piston from the drop in bleed plenum pressure that tends to close the valve. The shield pressure is ducted to the cowl surface near the inlet throat to improve response characteristics. The result is that the shielded valve opens farther than the unshielded valve for equal pressure steps. The response of the shielded valve is overdamped, and the valve will require no damping orifice.

The transient responses of both valves were compared with responses obtained with an analog computer simulation of the valve. Good agreement was obtained. The results indicated that the simulation can be used to predict response characteristics for the valves at varying wind tunnel and flight conditions.

INTRODUCTION

Mixed-compression supersonic inlets must operate with the terminal shock near the inlet throat in order to maintain high operating performance. If the terminal shock moves downstream, it occurs at a higher Mach number and thus increases the pressure losses across the shock. These increased losses result in low pressure recovery and high distortion at the engine face. With the shock near the throat, small changes in engine airflow or inlet capture airflow can create an inlet unstart in which the shock moves rapidly out of the inlet. The unstart is accompanied by a large reduction in airflow to the engine and a resulting reduction in engine thrust. This loss in thrust together with the drag created by the bow shock in front of the inlet cowl can cause large yawing and rolling moments on the aircraft with resulting difficulties in control, as described in reference 1.

Fixed-exit bleed systems that bypass air from the cowl throat region when the terminal shock goes into the throat region have been developed. They allow a certain amount of mismatch between the air captured by the inlet and that used by the engine. However, these bleed systems are passive and require a small but continual bleed flow even when the inlet is operated supercritically. To avoid large continuous airflows, the bleed exit orifice must be small. This limits the maximum amount of airflow these systems can bypass. Systems of this type are described in reference 2.

An active bleed system has been demonstrated that uses self-actuating relief valves to hold a constant pressure behind the bleed surface (refs. 2 to 4). This system can automatically bypass large amounts of air when required to prevent unstarts, but it operates with low leakage when the inlet is supercritical. Since this system was used to demonstrate the concept in a wind tunnel model, the valves were not designed to fit within the cowl of a flight weight inlet. They were also not designed to withstand the high temperatures encountered in high Mach number flight.

As a continuation of the active stability bleed effort a flight worthy system has been designed for the YF-12 aircraft. The relief valves for this system were constructed to operate in the high-temperature environment accompanying Mach 3 operation of the aircraft. The complete system can be incorporated into a full-scale YF-12 inlet model that can be tested in a wind tunnel.

Two prototypes of these relief valves were tested in a special dynamic valve test facility to (1) determine their dynamic response to steps in pressure at the face of the valves, (2) determine the effect of damping orifice diameter on the response of the valve under various operational conditions, and (3) verify that an analog computer simulation of the valve adequately duplicates the valve characteristics so that the simulation can be used to predict the valve performance under future wind tunnel and flight conditions. The analog simulation is described in appendix B. (Symbols are defined in appendix A.)

This report (1) describes the stability valve system and the construction of the relief valves, (2) describes the dynamic test facility and the procedure used to test the valves, (3) presents the results of the transient tests, and (4) compares the results of the transient tests with similar results of tests of simulated valves.

U. S. customary units were used in the design of the valves and for recording experimental data. The units were converted to the International System of Units for presentation in this report.

DESCRIPTION OF STABILITY BLEED SYSTEM

General Description

The stability bleed system designed for the YF-12 aircraft inlet is shown schematically in figure 1. The system consists of a porous bleed region in the cowl wall extending from 4.31 centimeters upstream of the inlet throat to 29.7 centimeters upstream of the throat. Fifty pressure relief valves, located circumferentially in two rows around the inlet, dump air overboard from the bleed cavity. Another porous bleed region is located on the spike and is at the same axial location as the cowl bleed when the spike is in the scheduled cruise position. This bleed region allows continuous bleed overboard.

The normal airflow control system on the YF-12 aircraft consists of automatically controlled forward bypass doors that dump inlet air overboard if the terminal shock goes forward of the operating point. If engine airflow increases and causes the shock to move downstream of the operating point, the doors tend to close and reduce the amount of air dumped overboard. The forward doors are supplemented by aft bypass doors that are used at flight Mach numbers that require large amounts of bypass air. These doors are operated by the pilot.

The stability bleed system is intended to augment the normal airflow bypass control system and extend the dynamic operating range of the overall control system beyond the capabilities of the present bypass control.

Relief Valves

The stability relief valves, shown installed in the YF-12 inlet in figures 2 and 3, remain closed for slowly changing disturbances. This is accomplished by means of an orifice in the piston face. For slow changes in bleed plenum pressure the air from the bleed plenum flows through the orifice into the spring and reference plenums, so that almost equal pressure is maintained in all chambers. The spring keeps the valves closed. However, if a fast change occurs in the bleed plenum pressure, the total orifice flow is

not large enough to prevent the valve from opening, and thus air is bled overboard from the bleed plenum.

The purpose of the damping orifice between the spring plenum and the reference plenum is to dampen the piston motion. Several damping orifice sizes were evaluated in the valve dynamic tests.

Two types of stability relief valves were built and tested. The first type is a conventional piston type relief valve (fig. 2). This valve senses the bleed plenum pressure directly and opens to maintain the bleed plenum pressure constant.

The second type of valve has a sensing duct and shield (fig. 3). The purpose of the duct and shield is to make the valve respond to the increase in inlet pressure as near the throat as possible and to remove the effective feedback force that the bleed plenum pressure applies to the piston face. Both of these effects tend to increase the speed of response of the valve to the terminal shock moving into the bleed region.

The two types of relief valves are shown in detail in schematic drawings in figure 4. The titanium piston is closely guided on the housing center post and there is generous clearance between the housing and the piston to prevent interference and binding. Leakage is controlled by two graphite piston rings. Bleed holes drilled between the piston rings help to minimize leakage from the spring plenum by reducing the pressure drop across the top ring so that it equals the difference between the pressure under the piston and the spring plenum pressure. Leakage across the bottom ring from the pressure under the piston to the atmosphere is not as important.

The bellmouth shape of the valve seat increases the flow coefficient of the valve. A transducer composed of strain gages mounted on a special fingered spring washer (inset in fig. 4(a)) measures the position of the piston. The spring produces a force on the fingers of the washer when the valve piston moves. The strain gages then respond to deflection of the fingers and produce a voltage in a Wheatstone bridge. This type of transducer is required because of the limitation on space in the spring chamber and because the measurement device must not alter the dynamic characteristics of the valve.

Two views of the shielded valve are shown in figure 5. The latch cable and wires were used in conducting the dynamic tests on the valve and are explained in the section APPARATUS. The disassembled valve is shown in figure 6. One of the strain gages used to measure piston position can be seen in the figure.

APPARATUS

Test Facility

The dynamic test facility for evaluating the stability relief valves is shown schematically in figure 7. A photograph of the facility is shown in figure 8. The facility is lo-

cated on top of the Lewis 10- by 10-Foot Supersonic Wind Tunnel so that the wind tunnel can be used as a low-pressure high-volume airflow source. The 15.24-centimeter-diameter outlet air line from the test facility runs through the tunnel ceiling just downstream of the test section. Pressures as low as 0.69 newton per square centimeter can be attained.

The test facility (fig. 7) consists of a 50.8-centimeter-diameter tank with a bulkhead dividing the tank into two main chambers. The stability relief valve is mounted on a third chamber, located in the center of the bulkhead. This chamber represents the bleed plenum. Airflow passes through a perforated plate before it reaches the valve. The plate is perforated with 0.317-centimeter-diameter holes, which create a 40-percent porosity.

All the tests were conducted with the downstream butterfly valve fully open to choke the flow across the relief valve. With the relief valve closed, the pressure in the upstream chamber is regulated by means of the inlet butterfly valve. The bypass orifices maintain a high steady-state flow rate through the facility in order to minimize the change in pressure in the upstream chamber when the relief valve opens. A large wooden bellmouth at the outlet of the tank minimizes pressure losses across the outlet. A 16 000-cubic-centimeter volume is connected to the valve shield to minimize the pressure change under the piston as the valve opens. A 1600-cubic-centimeter volume connected to the valve with a rubber vacuum hose serves as a reference plenum. Twenty-kilowatt heaters heat the incoming air to prevent freezing as the air expands through the valve.

To apply the equivalent of a step change in pressure to the valve, a cable is attached to the valve piston, a differential pressure is established across the valve piston, and then the cable to the piston is released. A pressure differential across the piston is applied by means of valves A and B in figure 7. The small airflow that leaks out of the shield plenum through the sealing ring is made up by allowing a small bleed from the atmosphere to enter the shield plenum through valve A. The pressure in the spring chamber is controlled to a value less than the pressure in the shield plenum by allowing air to bleed out of the spring chamber into the outlet line through valve B. The cable release mechanism is operated by a solenoid and is shown in figure 9. The latch cable from the valve piston is pinned to the stem of a weight holder. When the solenoid is activated, it pulls the release pin from the loop in the cable, the weights drop, and the piston is released.

The method of attaching the latch cable to the piston of the unshielded valve is shown in figure 10. Three wires are fastened in a groove in the piston. The loose ends are gathered together, wound around the latch cable, and crimped under a sleeve.

The latch cable of the shielded valve is attached as shown in figure 11. The latch wires pass through a special duct. The wires and disk have room to move within the duct a distance equal to the maximum piston stroke. The wires are soldered into holes in a

snap ring that fits the groove around the piston. The lower ends of the wires are soldered into three holes near the edge of the small brass disk. The latch cable is soldered into a hole in the center of the disk. The arrangement is shown in figure 12. Also shown in this figure are the graphite piston rings that minimize leakage from the valve spring chamber.

Instrumentation

The instrumentation used to conduct and evaluate dynamic performance tests on the stability relief valves is shown schematically in figure 7. The four pressure gages were used to set up conditions of the test prior to release of the piston. These gages are laboratory test gages with a vendor-advertized accuracy of 0.1 percent of full scale. Gages 1 and 2 have a range of 0 to 34.48 newtons per square centimeter, while gages 3 and 4 have a range of 0 to 17.24 newtons per square centimeter. Gages 1 and 2 were used to set up the pressure differential across the valve, while gages 3 and 4 were used to set up the pressure differential across the valve piston prior to release of the piston.

Three pressure transducers were installed in the facility to evaluate the performance data and to compare the data with the simulation results. These are high-response strain-gage transducers. A specially made position transducer, described in the section Relief Valves, was used to measure continually the position of the piston during the transient. The four variables of interest were recorded on a high-speed light beam strip-chart recorder.

TEST PROCEDURE

Friction Tests

Before the transient tests were run on each configuration, a determination of the frictional characteristics was made. This test, in addition to defining the friction force on the valve, provided a check of the initial spring force on the piston and the spring rate of the spring. These values were used in the valve simulation. The test was performed on the shielded valve by slowly applying a positive pressure on the sensing duct. This was done through valve A in figure 7. On the unshielded valve, a vacuum was applied to the reference plenum by disconnecting valve B. Valve position and pressure differential were plotted on an x, y-plotter as shown in figure 13. The valve did not open until both the spring force and friction were overcome. The spring rate was determined from the slope of the resulting curve and the piston area. When the valve was completely open, the pressure was gradually decreased. The width of the resulting hystere-

sis curve was used to determine the friction force. The friction curve for the unshielded valve is shown in figure 13, while the curve for the shielded valve is shown in figure 14.

Transient Tests

The tests described in this report were conducted to determine the dynamic response of the stability relief valve under a variety of pressure conditions within the limitations of the test facility. To perform the tests it was desirable to apply a step change in pressure to the face of the valve. Because of the difficulties of actually developing a step in pressure in a relatively large volume, an alternative method of applying the step was used. The piston was held in a closed position by the latch cable while a pressure differential was applied across the piston. The piston was then released. At the time the piston was released, the piston face pressure and the upstream chamber pressure were at the pressure immediately following the equivalent step. The spring and reference plenum pressures were at the pressure immediately preceding the step. After the valve opened, the pressure in the chamber that represented the bleed plenum dropped because of the pressure drop across the porous plate. The transient motion of the piston together with the three pressure transducer outputs were recorded.

RESULTS AND DISCUSSION

Table I lists the various valve configurations that were tested. The shielded valve was evaluated with springs having spring rates of 4.76 and 8.05 newtons per centimeter. Spring rates of 4.84 and 8.52 newtons per centimeter were evaluated in the unshielded valve. Damping orifice diameters of 0.508, 0.762, and 1.016 centimeter were tested with each valve. One additional test was made with one-half of the porous area upstream of the shielded valve blocked off. All valve configurations were evaluated with initial upstream chamber pressures of 0.95, 1.27, 1.59, and 2.46 newtons per square centimeter.

The results of the experimental program are presented in figures 15 to 25 in the form of valve piston transients resulting from the equivalent of steps in upstream chamber pressure. Figures 15 to 21 show transients produced with three orifice sizes and two upstream chamber pressure step sizes. Figures 22 to 25 show transients produced with two spring rates or two bleed areas and two upstream chamber pressure step sizes. Figures 26 to 33 present comparisons of the experimental data with simulated valve transients for one step size for each orifice diameter.

Effect of Damping Orifice

Unshielded valve. - Results of transient tests of the unshielded valve conducted with an initial pressure of 2.46 newtons per square centimeter are presented in figure 15. Figure 15(a) shows the response of piston position to a small (0.689-N/cm^2) pressure step, and figure 15(b) shows the piston transient caused by a larger (1.034-N/cm^2) pressure step. The test conducted with the largest (1.016-cm-diam) damping orifice resulted in a large overshoot of the piston. The smallest (0.508-cm-diam) orifice caused very little overshoot, but the piston opened more slowly. Piston transients obtained with a 0.762-centimeter-diameter orifice fell between the other two. This general trend held true for all of the unshielded valve transients. Piston transient curves for initial pressures of 1.59, 1.27, and 0.95 newtons per square centimeter are shown in figures 16, 17, and 18, respectively. The initial upstream chamber pressure had little effect on the test results. The results indicate that a damping orifice diameter of about 0.50 centimeter should be used.

Shielded valve. - Valve transient response tests on the shielded valve for initial pressures of 2.46, 1.59, and 1.27 newtons per square centimeter are shown in figures 19, 20, and 21, respectively. Again, for the shielded valve, the responses were generally the same for all initial pressure values. All responses were overdamped, and there was no overshoot. When the responses of the shielded valve are compared with those of the unshielded valve, two general observations can be made. First, the shielded valve was highly damped compared with the unshielded valve. Second, the piston in the shielded valve moved farther for the same size pressure step than the piston in the unshielded valve. These effects can be seen by comparing figure 21(b) with figure 17(a). The reason for both effects was that the shield removed the influence of the bleed plenum pressure from the piston motion. With the unshielded valve the drop in bleed plenum pressure when the valve opened effectively produced a force on the piston in a direction to close the piston. This force resulted in a reduced piston stroke and also in a reduction in the damping of the valve. No damping orifice will be required for the shielded valve.

Effect of Spring Rate

Unshielded valve. - The effect of installing a spring of lower spring rate on the response of the unshielded valve can be seen in figure 22. The effect of spring rate on the dynamic response of the valve was small because the change in the pressure force acting on the bottom of the piston due to movement of the valve was large compared with the spring rate.

Shielded valve. - Figure 23 shows the effect of reducing the spring rate on the piston response of the shielded valve. For the same size pressure step the piston merely moved farther with the lower spring rate. However, as shown in figure 23(b), for pressure steps that caused the same piston motion, the lower spring rate response was more highly damped.

Effect of Size of Porous Bleed Area

Tests were conducted to see how reducing the area of the porous bleed region affects the valve response. The effect can be seen in figures 24 and 25 for initial pressures of 2.46 and 1.59 newtons per square centimeter, respectively. The 0.762-centimeter-diameter damping orifice was used. The test was conducted on the unshielded valve only since this was the only configuration in which the response was affected by the bleed plenum pressure.

Figures 24 and 25 show the effect of reducing the bleed area by a factor of 2. The effect was not great, although the reduced area did add some damping to the piston response.

Simulation Comparison

Response tests were also conducted on an analog simulation of the stability relief valve. Conditions under which the tests were run were chosen to match the prototype valve test conditions and configurations. The spring opening force and spring rates were determined from the friction curves of figures 13 and 14. The damping orifice flow coefficients were chosen as 0.6. A more detailed description of the simulation and the effect of both wind tunnel and flight environments on valve performance is given in reference 5.

Some basic changes were made to the simulation described in reference 5 to make it represent the dynamic valve test facility rather than the bleed system in the inlet itself. These changes involved the addition of the upstream chamber of figure 7 and a different representation of the porous bleed. The porous plate was treated as an orifice; its flow coefficient was taken as 0.6 rather than as a variable with values given by the pressure-flow relation used in reference 5. The experimental bypass orifice flow was assumed to be choked and to have a flow coefficient of 0.6.

Unshielded valve. - Comparisons of the simulated transient responses with responses in tests of the unshielded valve are shown in figures 26 to 29. Figures 26 and 27 show responses to pressure steps of 1.034 and 0.689 newton per square centimeter, respectively. The initial pressure was 1.59 newtons per square centimeter for both. Re-

sults are shown in each figure for damping orifice diameters of 1.016, 0.762, and 0.508 centimeter. The simulated valve was always less damped than the prototype. This was probably due to the additional resistance of the connecting rubber tubing in series with the damping orifice. The resistance of the tubing was not considered in the simulation. Also, generally the piston stroke in the simulation did not settle out at as high a value as the prototype. The reason for this was not determined.

Similar comparisons are shown in figures 28 and 29 for an initial pressure of 1.27 newtons per square centimeter.

Shielded valve. - Transient responses for the simulated shielded valves are compared with the prototype responses in figures 30 and 31 for an initial pressure of 1.59 newtons per square centimeter and in figures 32 and 33 for an initial pressure of 1.27 newtons per square centimeter. The simulated responses followed the prototype responses quite closely. However, as with the unshielded valve, the simulated responses did not reach as high a final value after a step as did the prototype valve.

SUMMARY OF RESULTS

Dynamic tests were conducted on two prototype relief valves that were designed for use in a stability bleed system for a YF-12 flight inlet. The inlet was modified for wind tunnel evaluation. One of the valves was an unshielded direct-acting poppet valve. The other valve had a shield to isolate the bottom of the piston from the drop in bleed plenum pressure that would tend to close the valve. The results of these tests were used to verify that an analog simulation of the stability relief valves would adequately describe the dynamic behavior of the relief valve. The simulation is described in NASA TM X-3219.

A comparison of simulated transient responses with experimental test results for identical conditions indicated that the simulation adequately predicted the actual valve dynamic behavior and could be used to determine the dynamic behavior of the valve for a variety of wind tunnel and flight conditions.

The experimental data also confirmed the findings of the simulation program, that no damping orifice will be required on the shielded valve. However, the unshielded valve will require a 0.50-centimeter-diameter orifice to reduce large overshoots in piston response following changes in pressure on the piston face.

Of the two springs tried with the shielded valve, the lower rate (4.76 N/cm) resulted in the valve opening faster and farther for the same pressure step size than the higher rate (8.05 N/cm). The effect of changing the spring rate in the unshielded valve was small.

The absolute pressure level had little effect on the valve response for either valve.

Decreasing the porous bleed area of the unshielded valve by a factor of 2 resulted in only slight damping of the valve.

Lewis Research Center,
National Aeronautics and Space Administration,
Cleveland, Ohio, April 22, 1975,
743-03.

APPENDIX A

SYMBOLS

A	area, cm^2
A_v	area of piston at seat, cm^2
C	pneumatic capacitance, $(cm^2)(kg)/N$
C_f	flow coefficient
D_v	valve piston diameter, cm
F	force, N
g	gravitational constant, 100 $(kg)(cm)/(N)(sec^2)$
K	spring rate, N/cm
M	mass, kg
$\dot{m}$	mass flow rate, kg/sec
P	pressure, N/cm^2
$\dot{P}$	rate of change in pressure with respect to time, $(N/cm^2)/sec$
R	gas constant, 28 700 (cm)(N)/(kg)(K)
T	temperature, K
V	volume, cm^3
x	piston position, cm
$\dot{x}$	piston velocity, cm/sec
$\ddot{x}$	piston acceleration, cm/sec^2
γ	ratio of specific heats
ρ	density, kg/cm^3

Subscripts:

a	reference volume
b	bleed plenum
by	bypass orifice
c	spring plenum
fl	flow
o	piston face orifice

p shield plenum

r friction

sp spring

v valve

x upstream chamber of test facility

APPENDIX B

ANALOG SIMULATION OF A DIRECT-ACTING POPPET RELIEF VALVE

The simple direct-acting poppet relief valve used in the YF-12 shock stability system program was simulated on a general purpose electronic analog computer. A complete description of the simulation and a study of valve dynamic behavior under various wind tunnel and flight conditions are presented in reference 5. The general equations as presented in reference 5, as well as changes made to the equations to make them describe the dynamic test facility, are presented in this appendix.

Unshielded Valve Equations

Dynamic force equation. - The basic equation that determines the piston position x is obtained by equating all forces that act on the piston to zero. Positive forces are assumed to act downward, and positive motion is assumed to be in the direction of opening the valve or upward (see fig. 34). The force equation is

$$M\ddot{x} + P_cA_v - P_bA_v + F_{fl} + Kx + F_{sp} + F_r(\mathrm{sgn}\ \dot{x}) = 0 \tag{B1}$$

where

$M\ddot{x}$	force due to accelerating mass of piston
P_cA_v, P_bA_v	pressure forces acting on piston area
F_{fl}	flow force acting on piston; force was obtained experimentally on one-sixth scale model of piston
Kx	force due to compressing spring through distance x
F_{sp}	initial spring force set on spring
$F_r(\mathrm{sgn}\ \dot{x})$	friction force on piston caused by sealing piston rings and by center support; force is assumed to be constant and to act upward when piston motion is downward and downward when piston motion is upward

Continuity equation for flow into upstream chamber. - The continuity equation for flow into the upstream chamber of the test facility is

$$C_x\dot{P}_x = \dot{m}_x - \dot{m}_{by} - \dot{m}_b \tag{B2}$$

where

C_x pneumatic capacitance of upstream chamber volume, equal to $V_x/\gamma RT$ for isentropic process

$C_x\dot{P}_x$ storage term for upstream chamber volume

$\dot{m}_x$ flow through inlet valve; flow is choked and therefore constant

$\dot{m}_{by}$ flow through bypass orifices; flow is assumed to be choked orifice flow

$\dot{m}_b$ flow through porous bleed region into bleed plenum

The flow $\dot{m}_b$ is assumed to be incompressible and can be expressed as

$$\dot{m}_b = A_b C_f \sqrt{2g\rho_x \left|(P_x - P_b)\right|}\ [\mathrm{sgn}(P_x - P_b)] \tag{B3}$$

where C_f is a constant equal to 0.6 and ρ_x is calculated at the P_x condition after the step is applied.

Continuity equation for flow into bleed plenum. - The continuity equation for flow into the bleed plenum can be expressed as

$$C_b\dot{P}_b = \dot{m}_b - \dot{m}_v - \dot{m}_o - A_v\rho_b\dot{x} \tag{B4}$$

where

$\dot{m}_v$ flow through metering portion of valve; flow is assumed to be choked since exit pressure is assumed to be wind tunnel static pressure

$\dot{m}_o$ flow through piston face orifice (with area A_o) to maintain P_c equal to P_b for steady-state conditions; flow is set equal to zero for comparison with actual tests

$A_v\rho_b\dot{x}$ equivalent flow from volume V_b due to piston motion; ρ_b is assumed constant and is calculated for P_b initial conditions before step in pressure is applied

The flow $\dot{m}_v$ is given by

$$\dot{m}_v = \frac{0.0400\ C_f P_b \pi D_v x}{\sqrt{T}} \tag{B5}$$

where C_f is a nonlinear function of the piston stroke; it was determined experimentally on the one-sixth scale model of the piston.

Continuity equation for flow into spring plenum. - Similarly, the continuity equation for flow into V_c may be written

$$C_c\dot{P}_c = \dot{m}_o + A_v\rho_c\dot{x} - \dot{m}_a \tag{B6}$$

where

$$\dot{m}_a = A_a C_f \sqrt{2g\rho_c\left|(P_c - P_a)\right|}\ [\mathrm{sgn}(P_c - P_a)] \tag{B7}$$

The capacitance of the spring chamber C_c decreases as the piston moves up:

$$C_c = \frac{V_c}{\gamma RT}$$

$$V_c = V_{initial} - A_v x$$

Continuity equation for flow into reference plenum. - Also, the continuity equation for flow into the reference volume may be written

$$C_a\dot{P}_a = \dot{m}_a \tag{B8}$$

Shielded Valve Equations

The basic simulation used to study the dynamics of the unshielded valve was used for the shielded valve with a few modifications to the equations (see fig. 35). The most important change is that the bleed pressure P_b no longer acts on the piston face. A new expression must be written to describe the forces that act on the piston. This new equation is

$$M\ddot{x} + P_cA_v - P_pA_v + F_{fl} + Kx + F_{sp} + F_r(\mathrm{sgn}\ \dot{x}) = 0 \tag{B9}$$

where P_pA_v is the new pressure force that replaces P_bA_v of equation (B1). During the transient tests P_p was held constant.

The continuity equation for flow into the bleed plenum must be rewritten for the shielded valve to remove the expressions for equivalent flow due to piston motion and flow through orifice A_o. The equation becomes

$$C_b\dot{P}_b = \dot{m}_b - \dot{m}_v$$

REFERENCES

1. Berry, D. T.; and Gilyard, G. B.: Some Stability and Control Aspects of Airframe/Propulsion System Interactions on the YF-12 Airplane. ASME Paper 73-WA/Aero-4, Nov. 1973.
2. Sanders, Bobby W.; and Mitchell, Glenn A.: Increasing the Stable Operating Range of a Mach 2.5 Inlet. AIAA Paper 70-686, June 1970.
3. Sanders, Bobby W.; and Mitchell, Glenn A.: Throat-Bypass Bleed Systems for Increasing the Stable Airflow Range of a Mach 2.50 Axisymmetric Inlet with 40-Percent Internal Contraction. NASA TM X-2779, 1973.
4. Mitchell, Glenn A.; and Sanders, Bobby W.: Pressure-Activated Stability-Bypass-Control Valves to Increase the Stable Airflow Range of a Mach 2.5 Inlet with 40-Percent Internal Contraction. NASA TM X-2972, 1974.
5. Webb, John A., Jr.; and Dustin, Miles O.: Analysis of a Stability Valve System for Extending the Dynamic Range of a Supersonic Inlet. NASA TM X-3219, 1975.

TABLE I. - VALVE CONFIGURATIONS

TESTED DURING DYNAMIC

EVALUATION OF STABILITY

RELIEF VALVES

Valve	Spring rate, N/cm	Damping orifice diameter, cm	Porous area, cm^2
Shielded	8.05	1.016 .762 .508	142
	4.76	1.016 .762 .508	142
Unshielded	8.52	1.016 .762 .508	142
	4.84	1.016 .762 .508	142
Unshielded	8.52	0.762	71

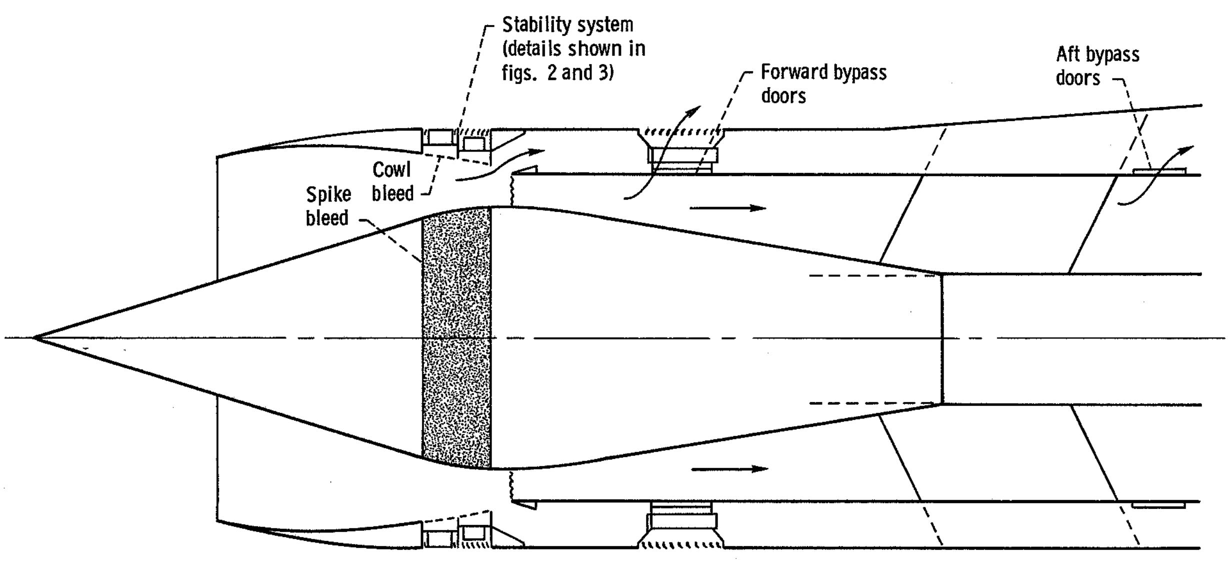

Figure 1. - YF-12 inlet with stability system.

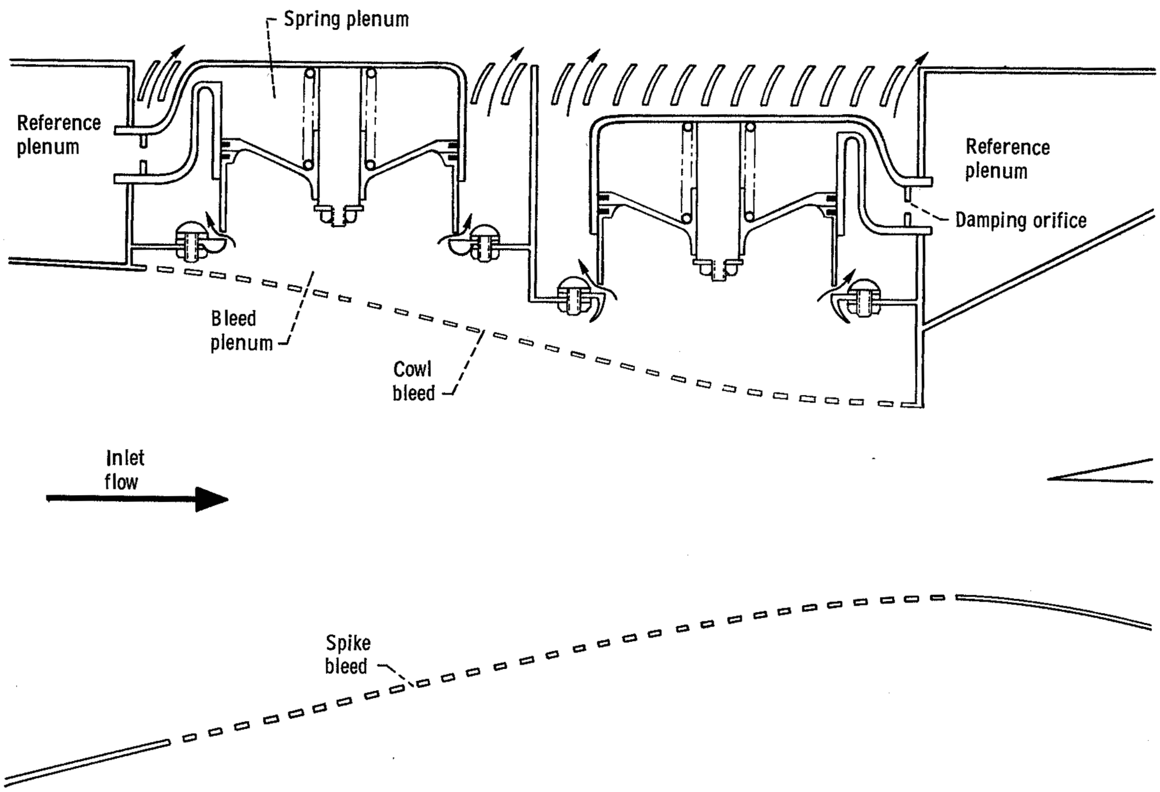

Figure 2. - Stability system with unshielded relief valves installed in YF-12 inlet.

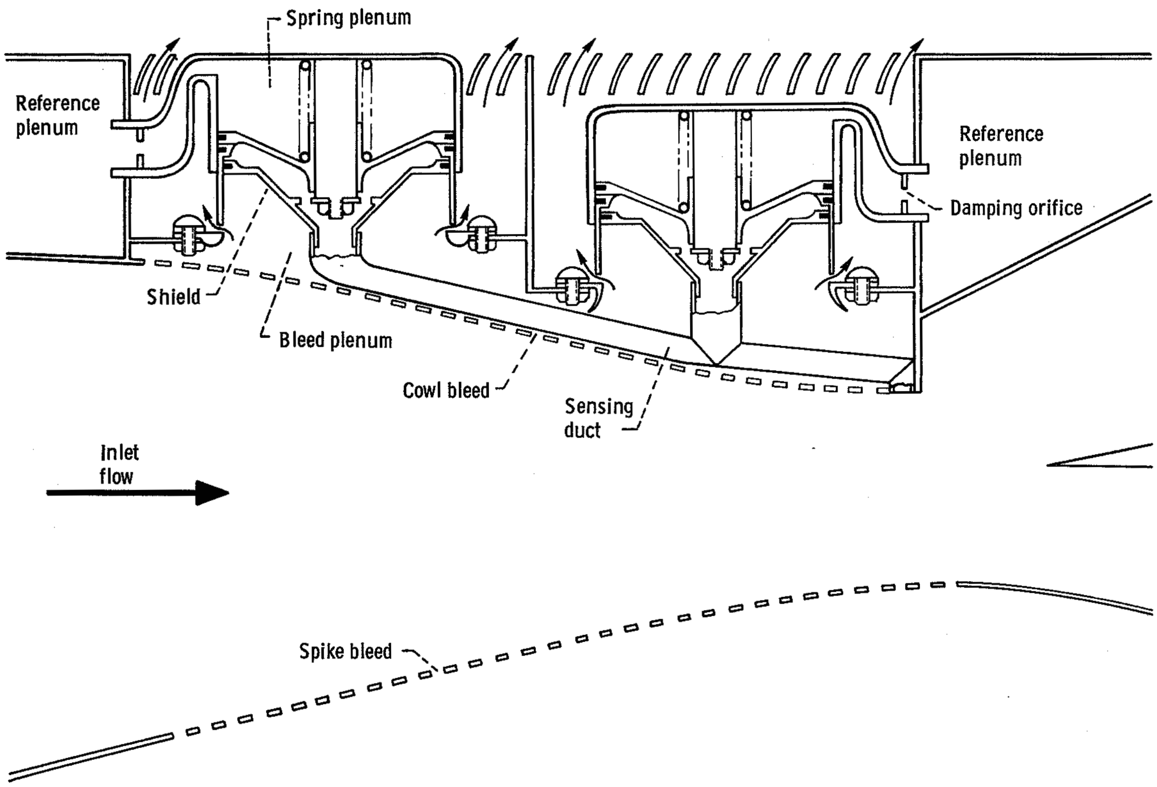

Figure 3. - Stability system with shielded relief valves installed in YF-12 inlet.

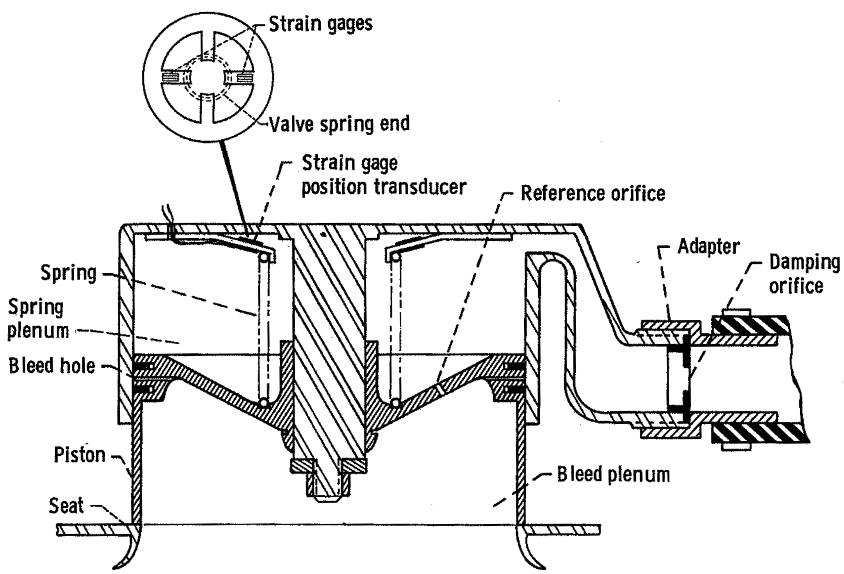

(a) Unshielded valve.

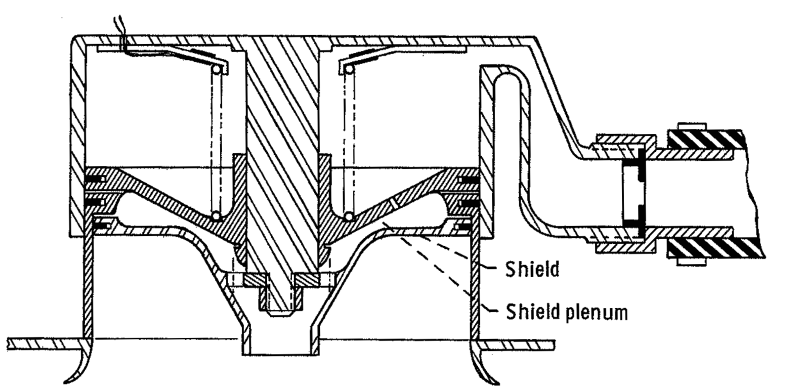

(b) Shielded valve.

Figure 4. - Stability system relief valves.

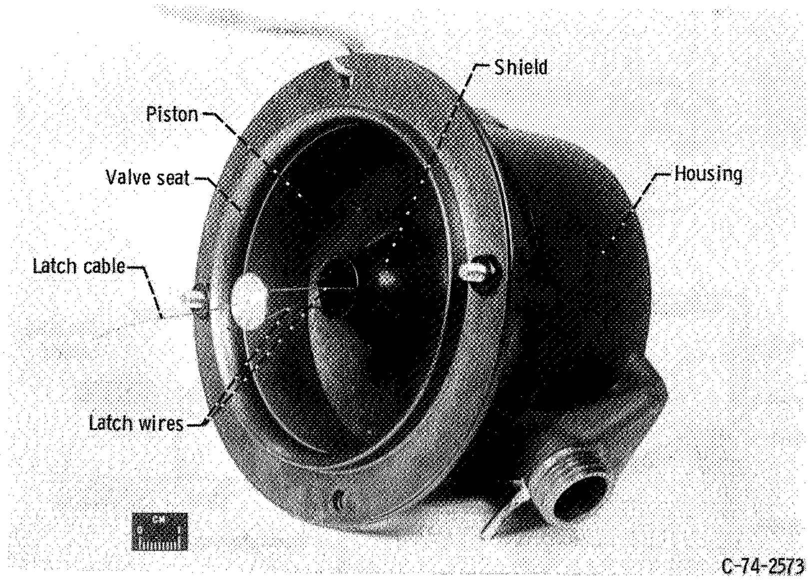

(a) Bottom view.

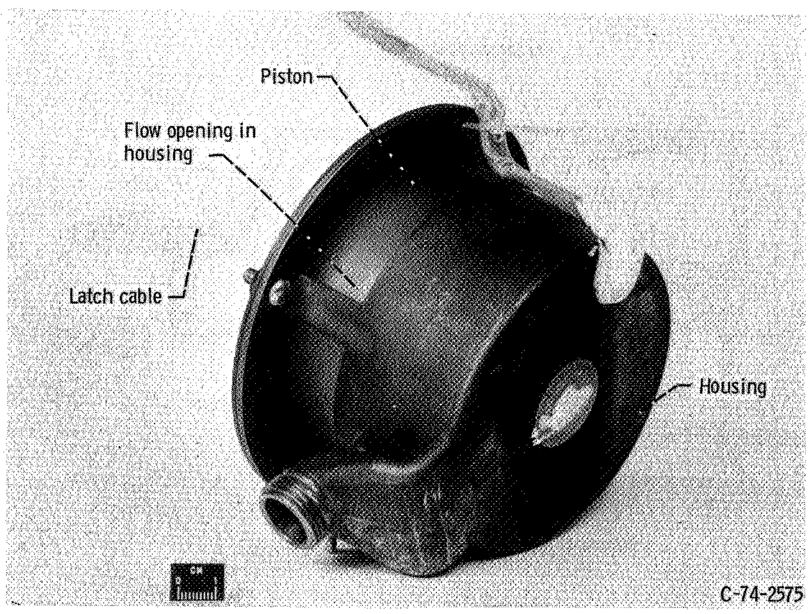

(b) Top view.

Figure 5. - Stability system relief valve assembled.

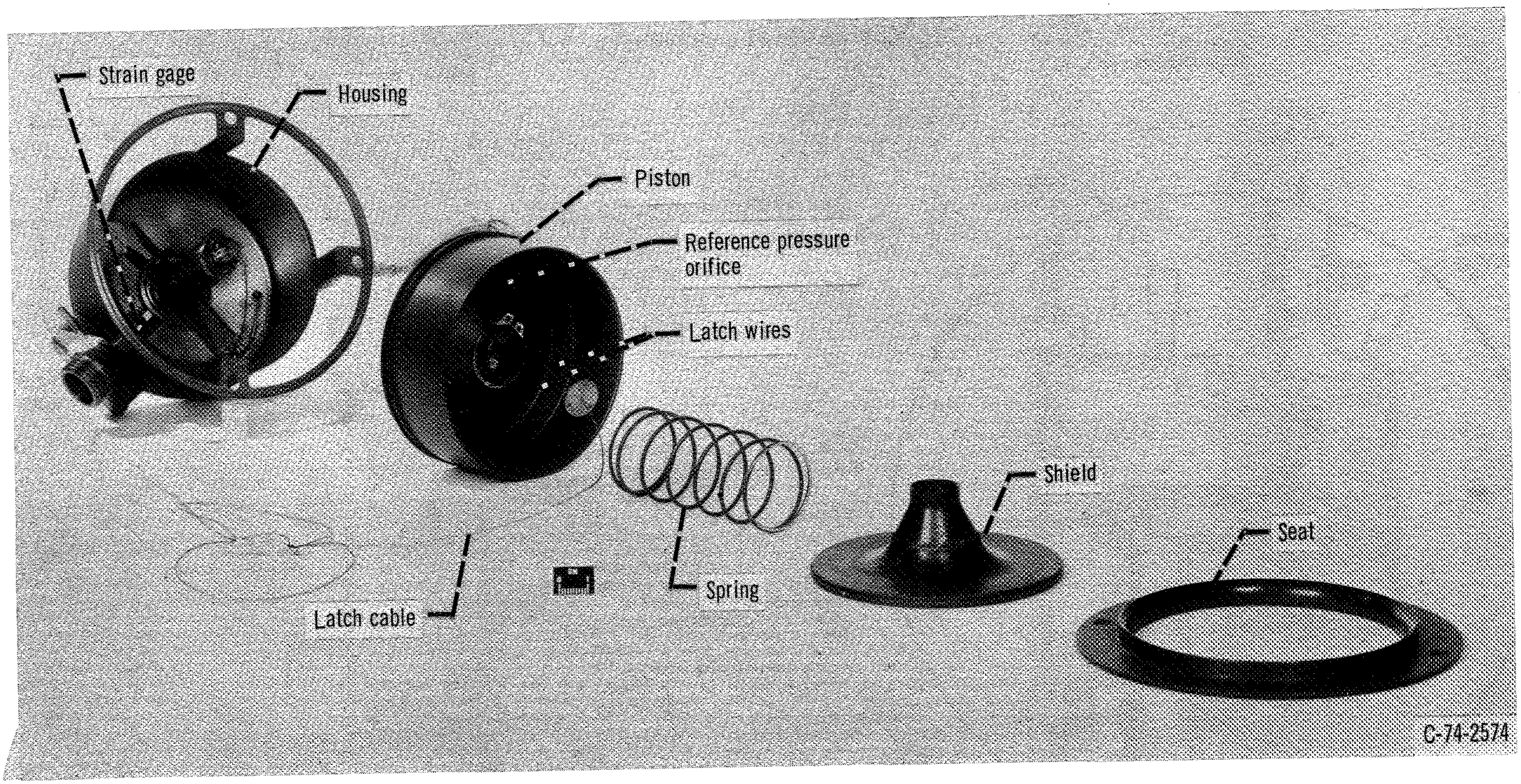

Figure 6. - Disassembled stability system relief valve.

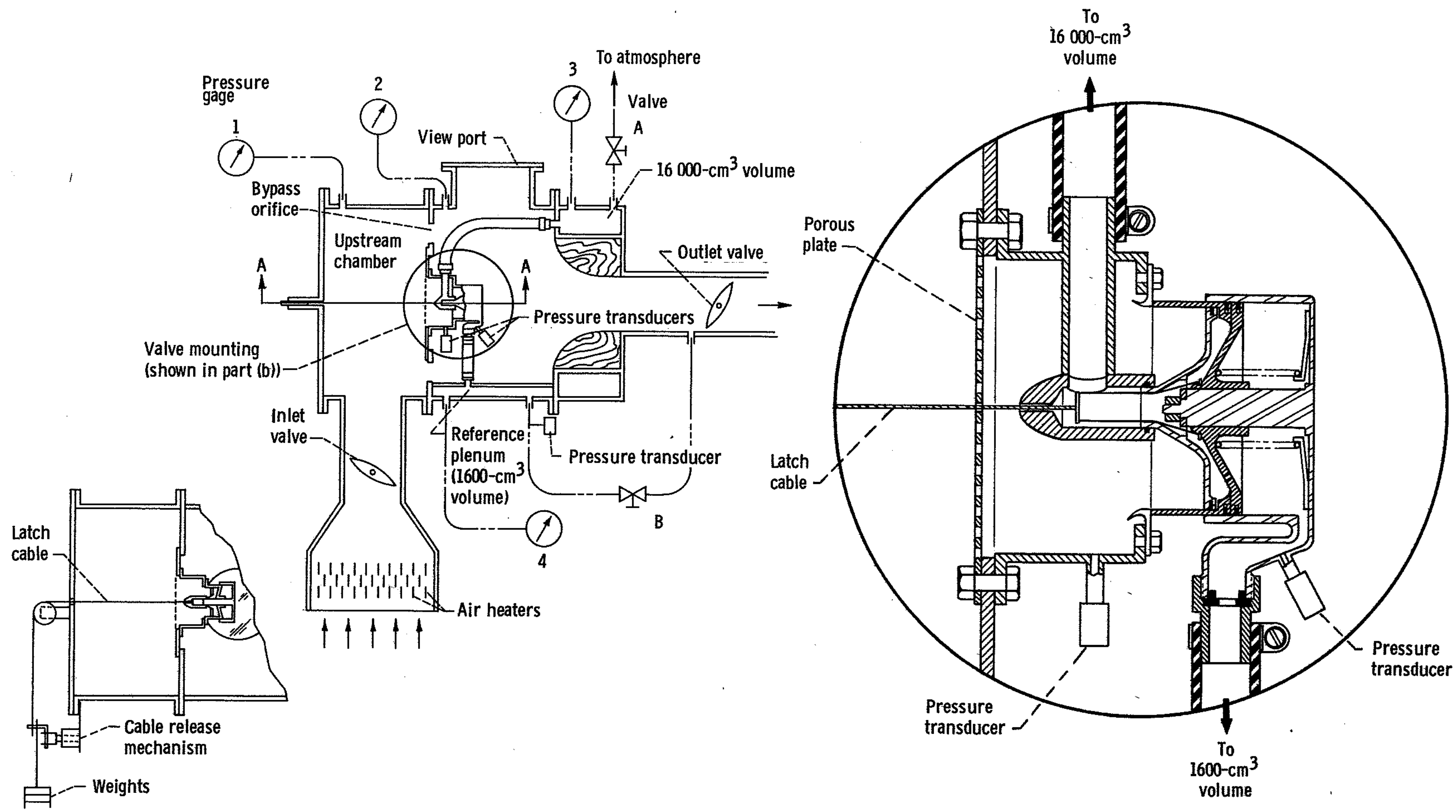

Section A-A

(a) Top view.

(b) Valve mounting.

Figure 7. - Relief valve test facility.

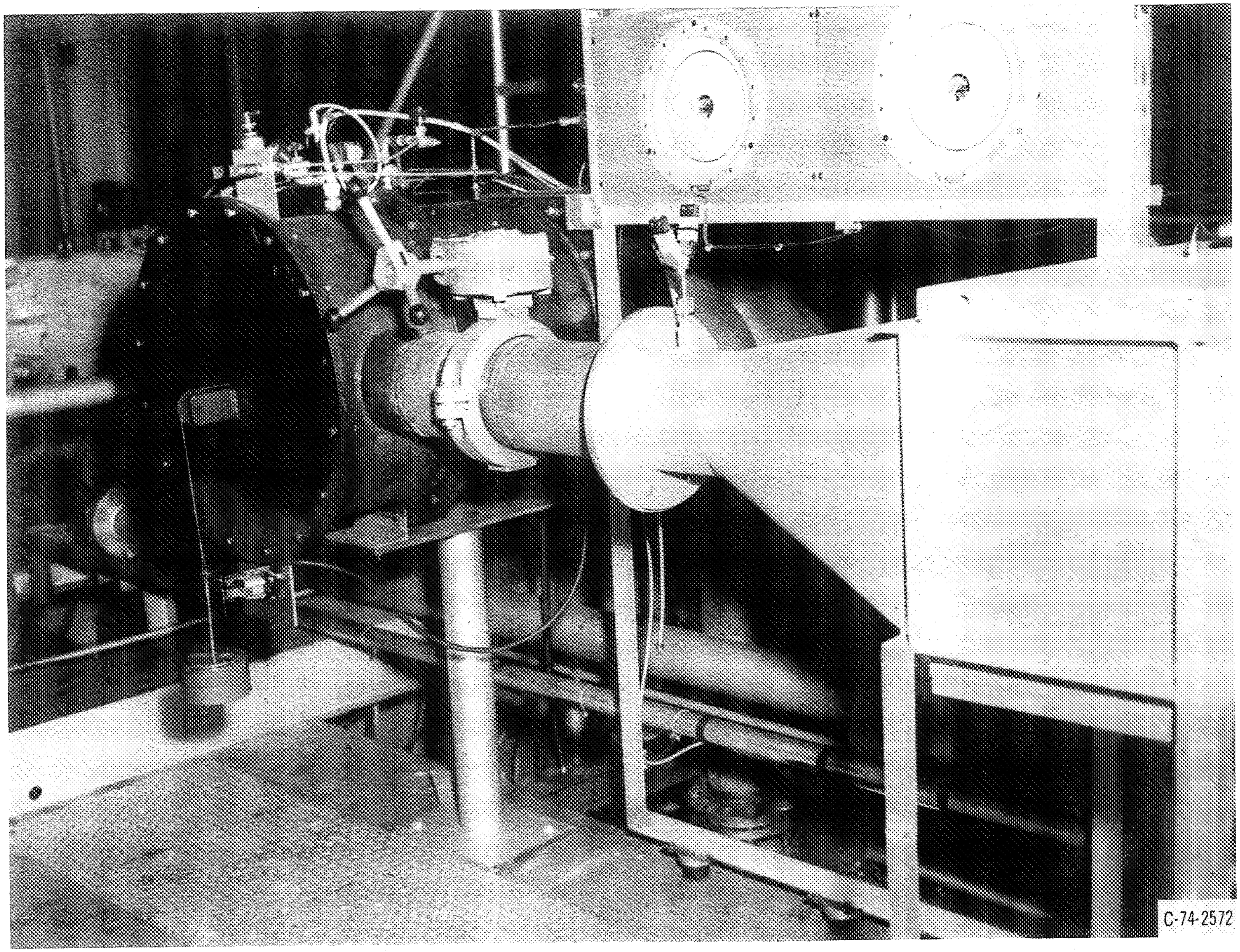

Figure 8. - Stability system relief valve test facility.

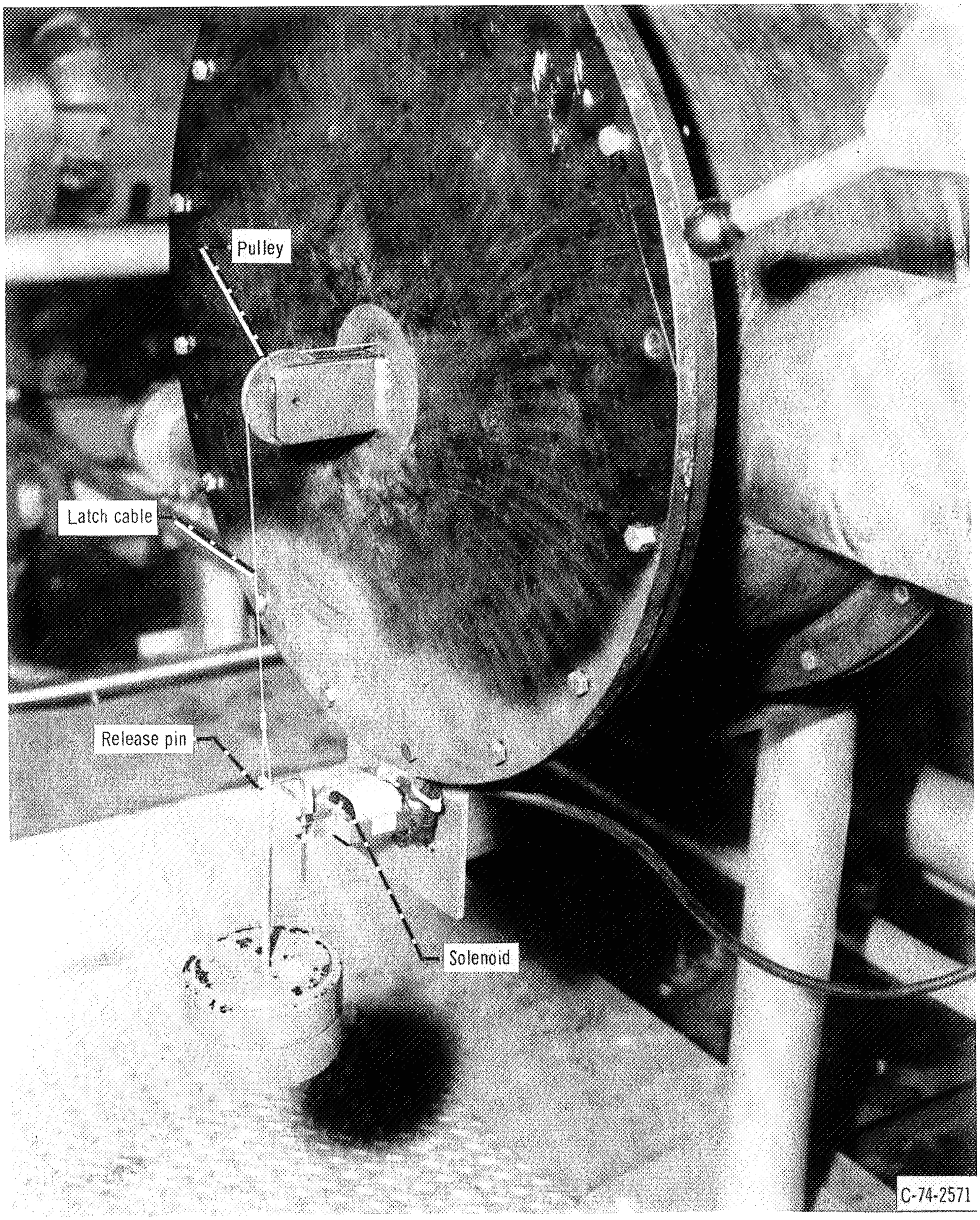

Figure 9. - Weight release mechanism.

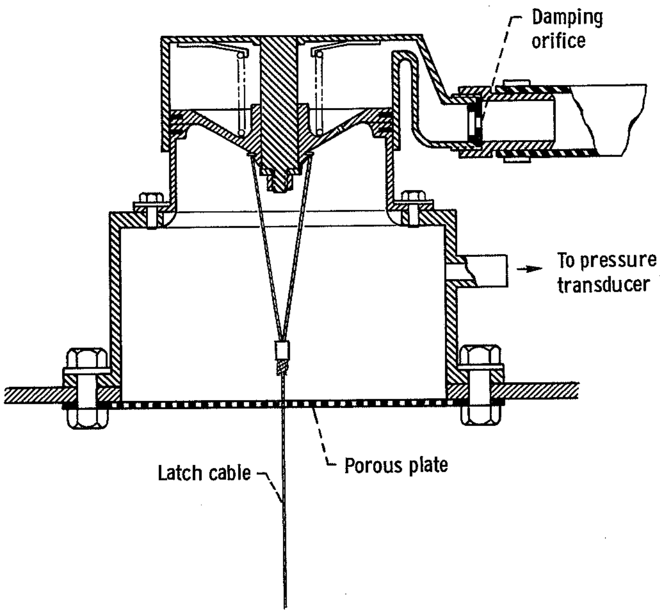

(a) Valve mounted in test facility.

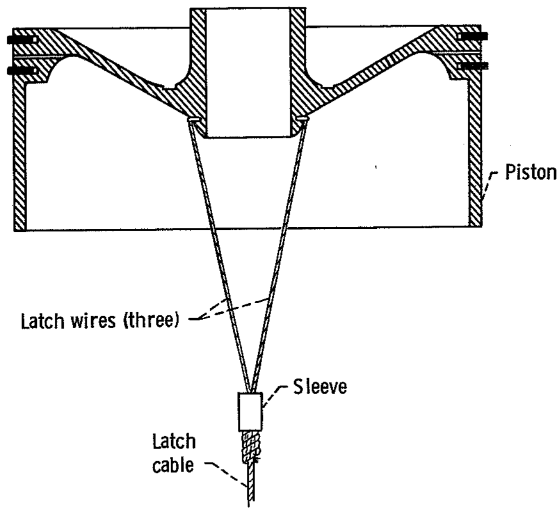

(b) Method of attaching latch cable to piston of valve.

Figure 10. - Details of installation of unshielded relief valve in test facility.

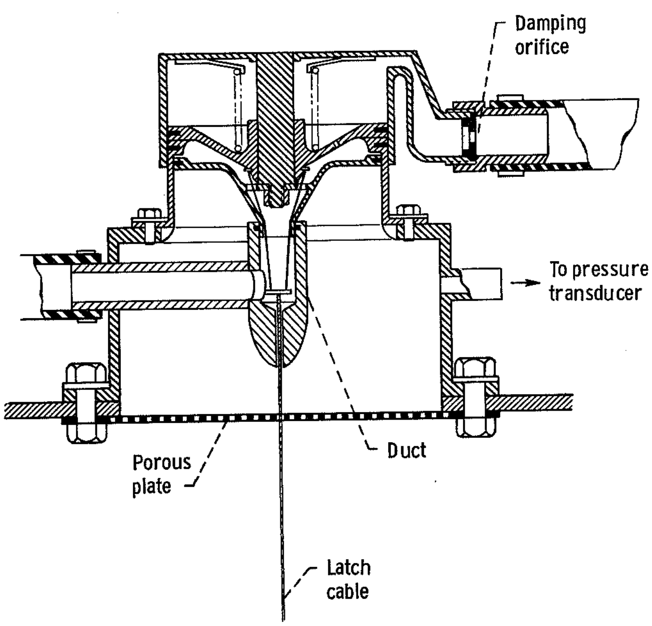

(a) Valve mounted in test facility.

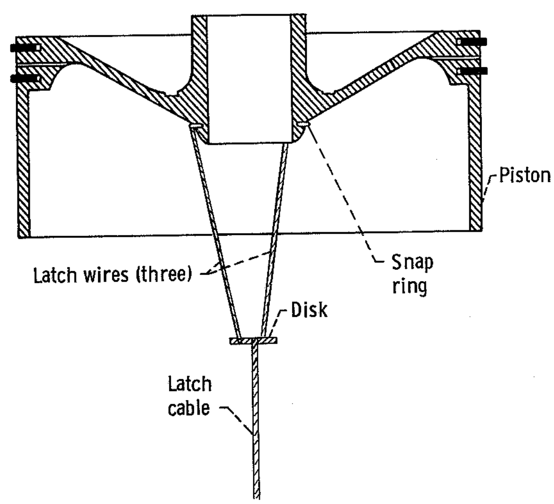

(b) Method of attaching latch cable to piston of valve.

Figure 11. - Details of installation of shielded relief valve in test facility.

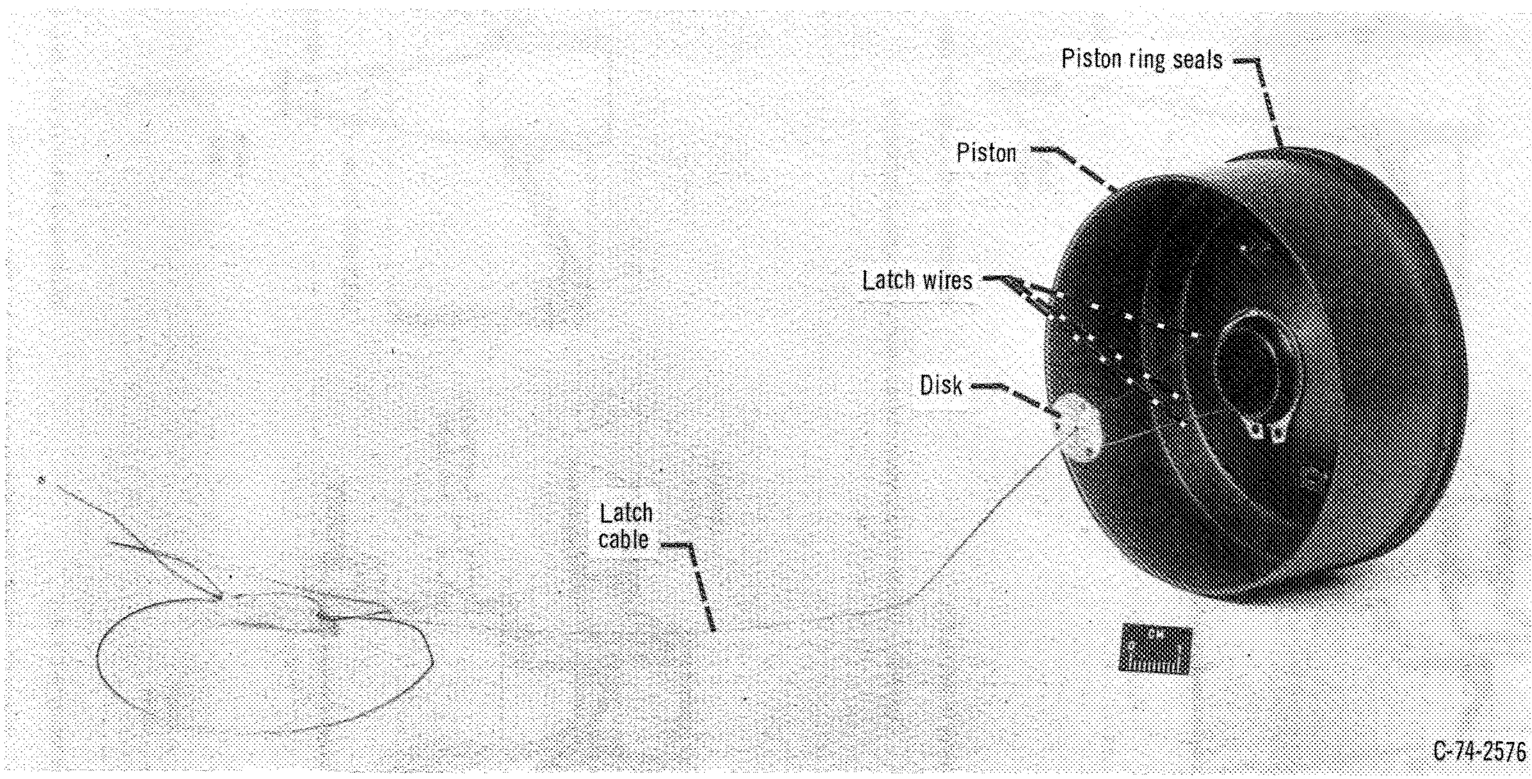

Figure 12. - View of stability system relief valve piston showing attachment of latch wires.

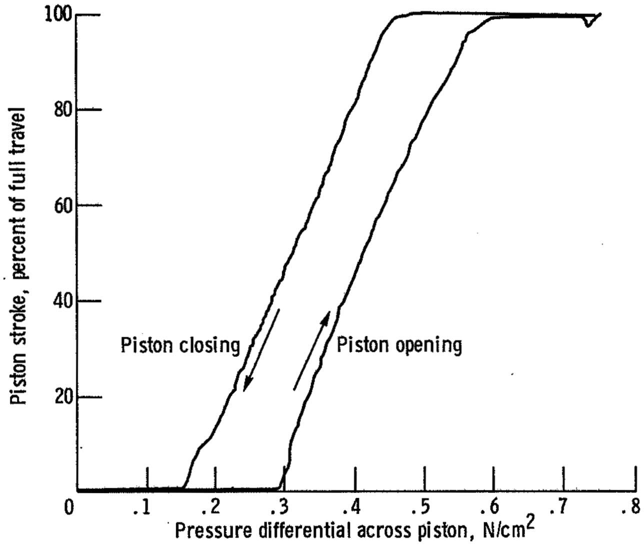

Figure 13. - Plot of piston stroke as function of differential pressure across piston showing friction hysteresis loop for unshielded relief valve. Average friction, ±3.91 newtons.

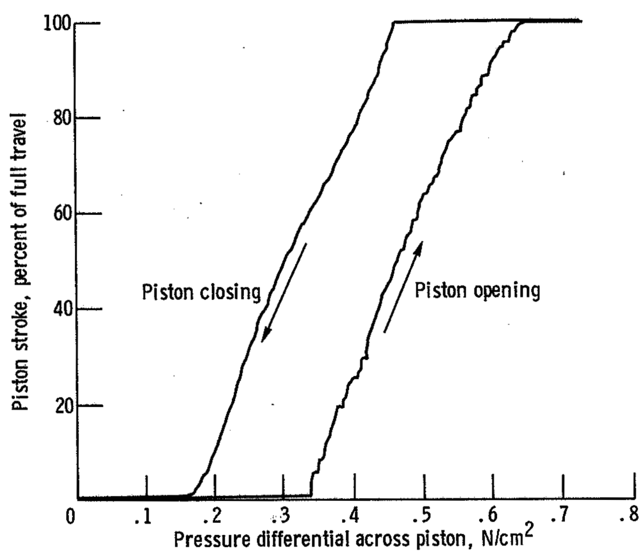

Figure 14. - Plot of piston stroke as function of differential pressure across piston showing friction hysteresis loop for shielded relief valve. Average friction, ±4.89 newtons.

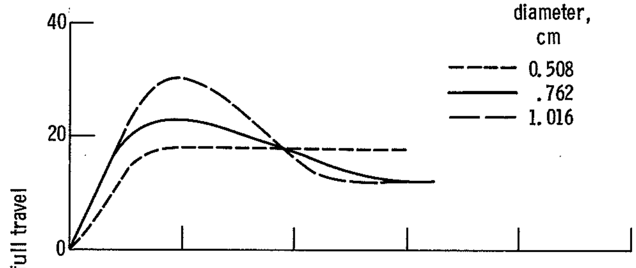

(a) Step size, 0.689 newton per square centimeter.

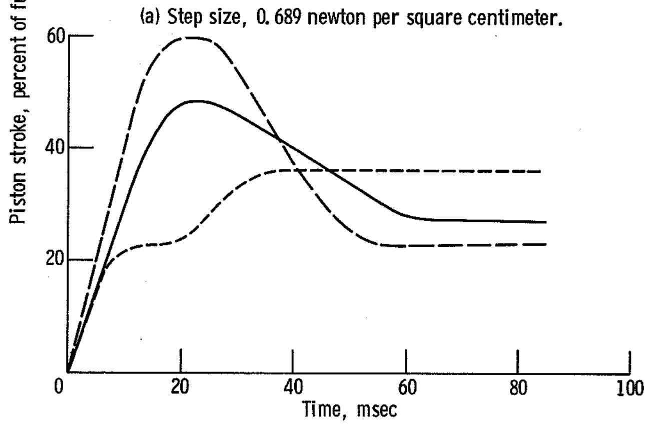

(b) Step size, 1.034 newtons per square centimeter.

Figure 15. - Effect of damping orifice size on unshielded relief valve response. Initial upstream chamber pressure, 2.46 newtons per square centimeter; spring rate, 8.52 newtons per centimeter.

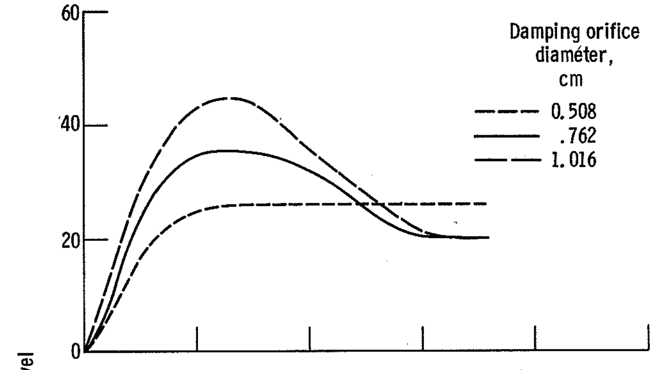

(a) Step size, 0.689 newton per square centimeter.

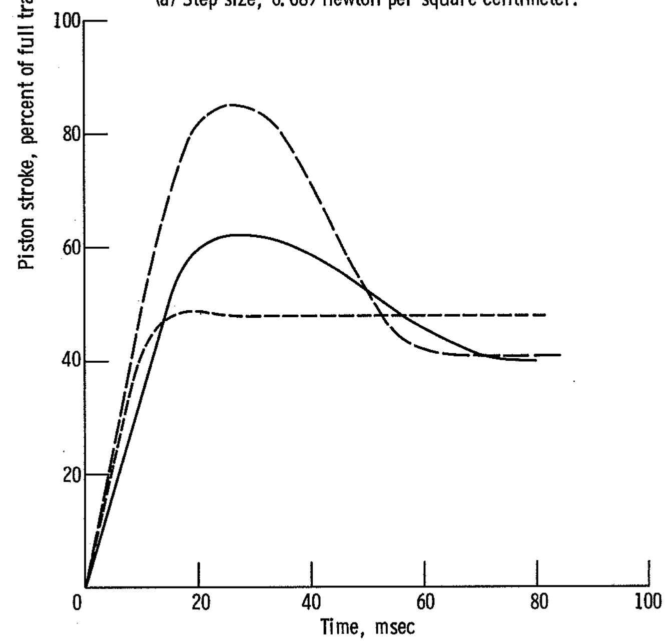

(b) Step size, 1.034 newtons per square centimeter.

Figure 16. - Effect of damping orifice size on unshielded relief valve response. Initial upstream chamber pressure, 1.59 newtons per square centimeter; spring rate, 8.52 newtons per centimeter.

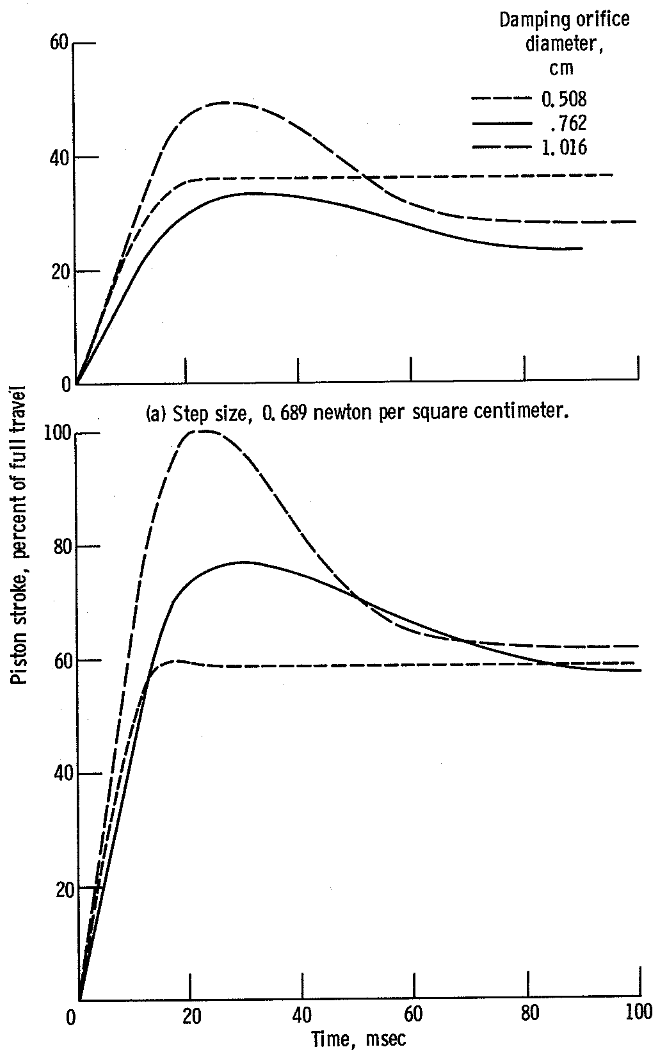

(a) Step size, 0.689 newton per square centimeter.

(b) Step size, 1.034 newtons per square centimeter.

Figure 17. - Effect of damping orifice size on unshielded relief valve response. Initial upstream chamber pressure, 1.27 newtons per square centimeter; spring rate, 8.52 newtons per centimeter.

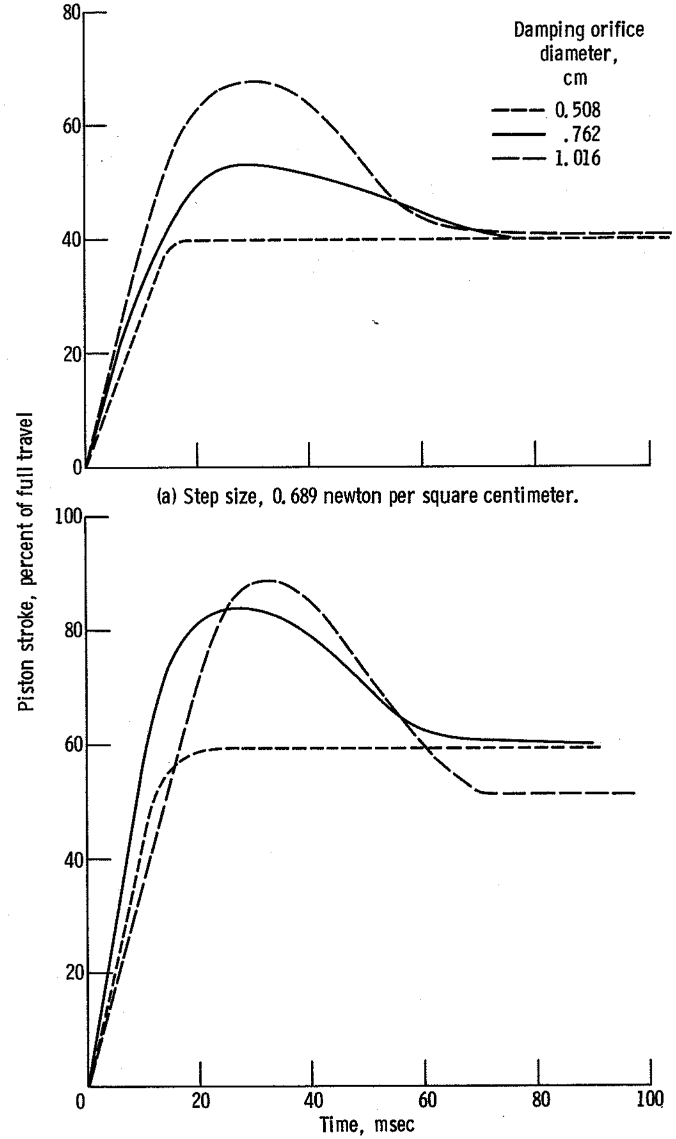

(a) Step size, 0.689 newton per square centimeter.

(b) Step size, 1.034 newtons per square centimeter.

Figure 18. - Effect of damping orifice size on unshielded relief valve response. Initial upstream chamber pressure, 0.95 newton per square centimeter; spring rate, 8.52 newtons per centimeter.

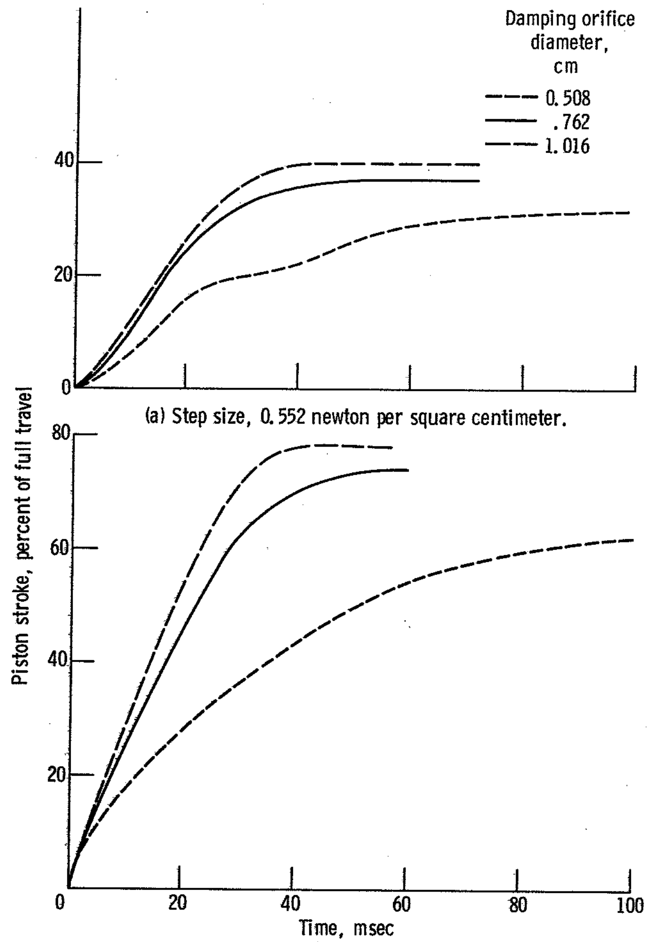

(a) Step size, 0.552 newton per square centimeter.

(b) Step size, 0.758 newton per square centimeter.

Figure 19. - Effect of damping orifice size on shielded relief valve response. Initial upstream chamber pressure, 2.46 newtons per square centimeter; spring rate, 8.05 newtons per centimeter.

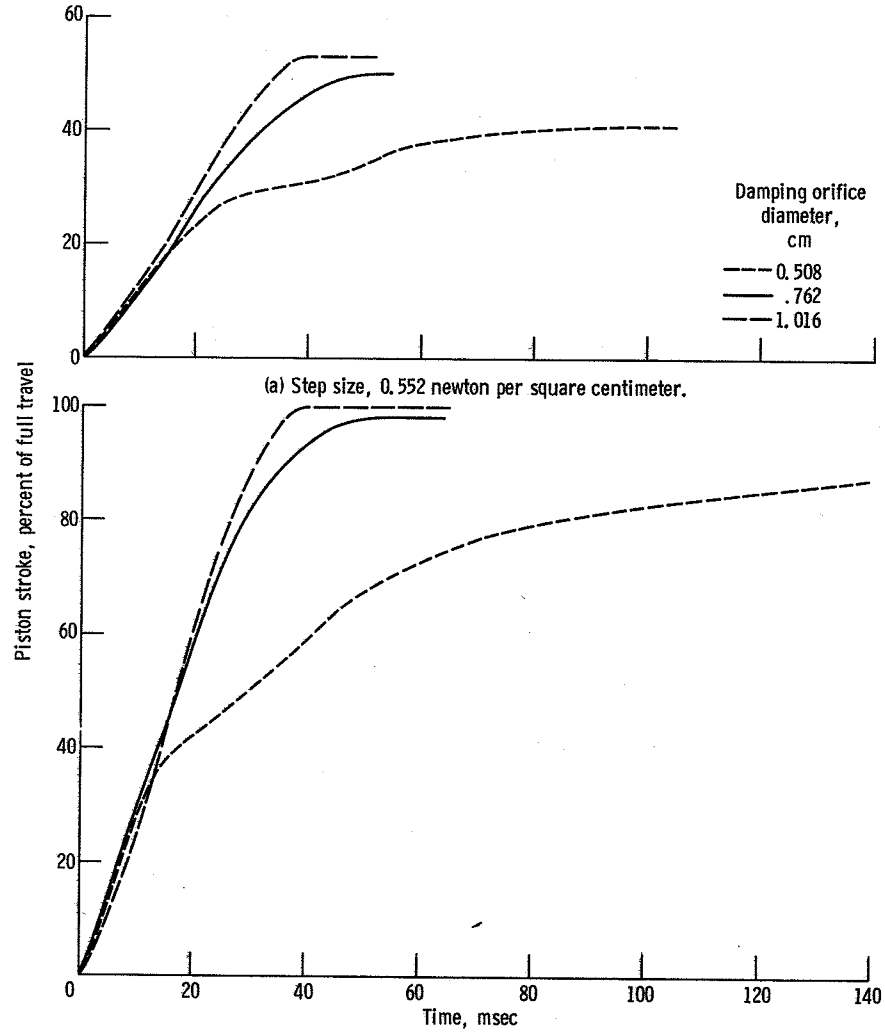

(a) Step size, 0.552 newton per square centimeter.

(b) Step size, 0.758 newton per square centimeter.

Figure 20. - Effect of damping orifice size on shielded relief valve response. Initial upstream chamber pressure, 1.59 newtons per square centimeter; spring rate, 8.05 newtons per centimeter.

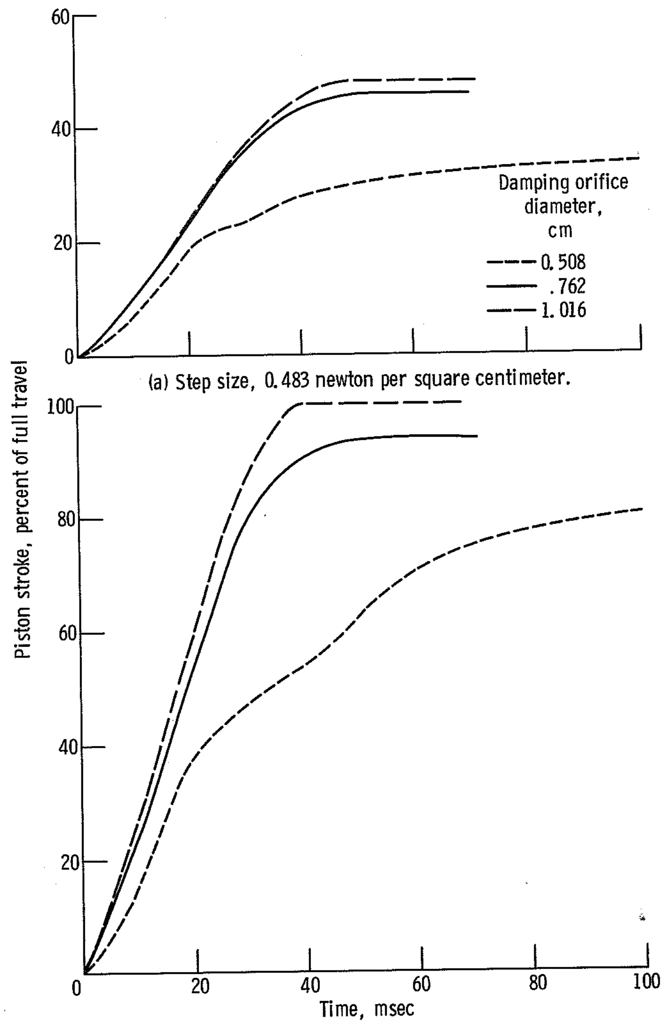

(a) Step size, 0.483 newton per square centimeter.

(b) Step size, 0.689 newton per square centimeter.

Figure 21. - Effect of damping orifice size on shielded relief valve response. Initial upstream chamber pressure, 1.27 newtons per square centimeter; spring rate, 8.05 newtons per centimeter.

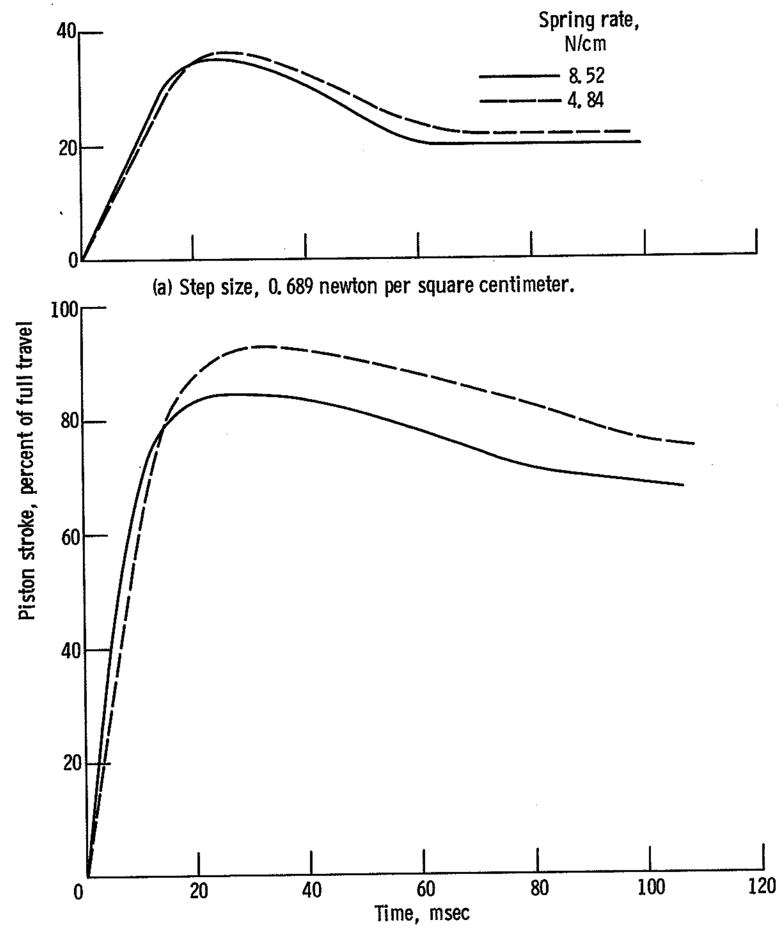

(a) Step size, 0.689 newton per square centimeter.

(b) Step size, 1.378 newtons per square centimeter.

Figure 22. - Effect of sping rate on unshielded relief valve response. Initial upstream chamber pressure, 1.59 newtons per square centimeter; damping orifice diameter, 0.762 centimeter.

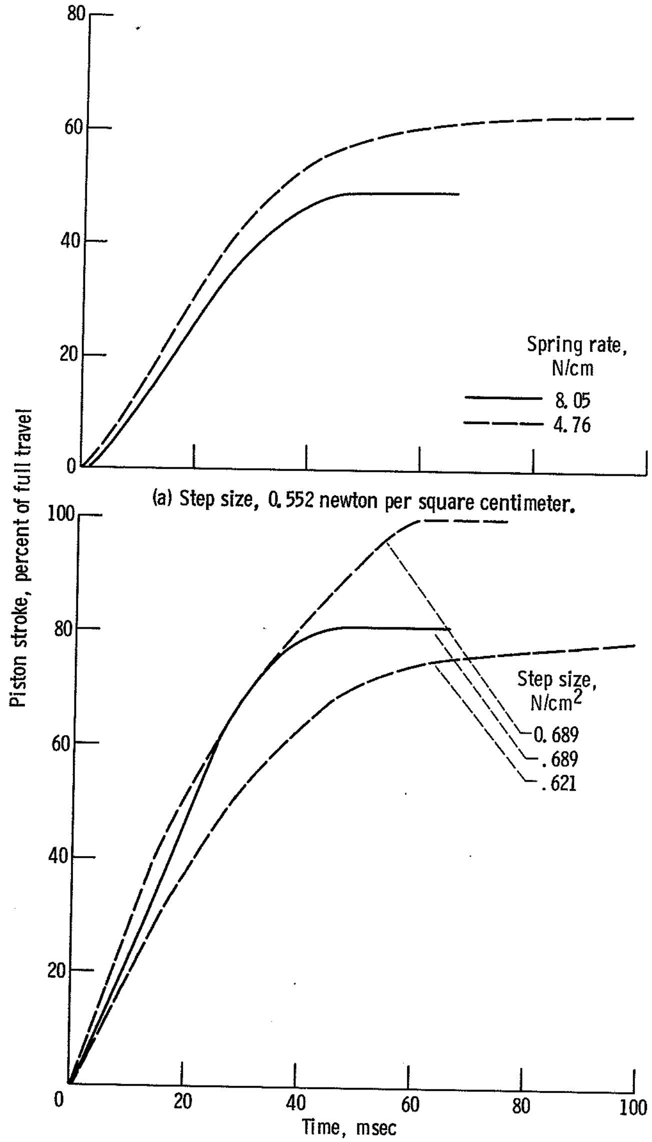

(a) Step size, 0.552 newton per square centimeter.

(b) Step sizes, 0.689 and 0.621 newton per square centimeter.

Figure 23. - Effect of spring rate on shielded relief valve response. Initial upstream chamber pressure, 1.59 newtons per square centimeter; damping orifice diameter, 0.762 centimeter.

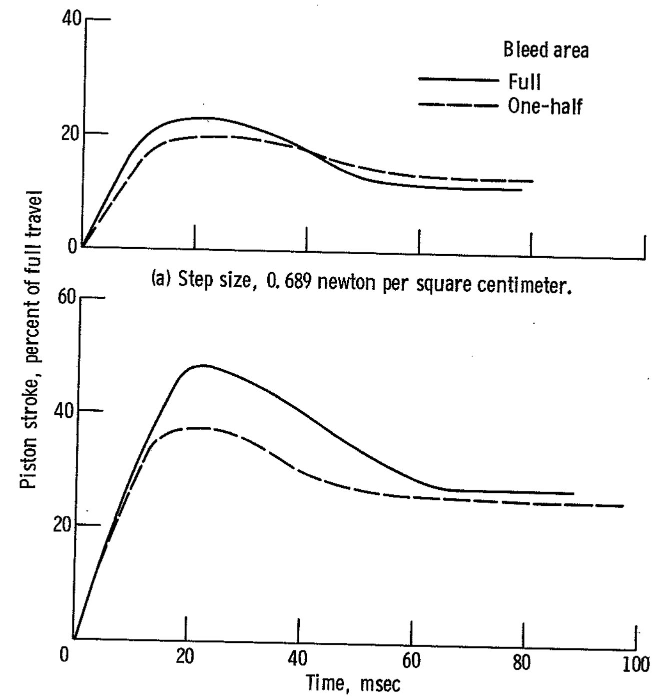

(a) Step size, 0.689 newton per square centimeter.

(b) Step size, 1.034 newtons per square centimeter.

Figure 24. - Effect of size of porous bleed area on response of unshielded relief valve. Initial upstream chamber pressure, 2.46 newtons per square centimeter; spring rate, 8.52 newtons per centimeter; damping orifice diameter, 0.762 centimeter.

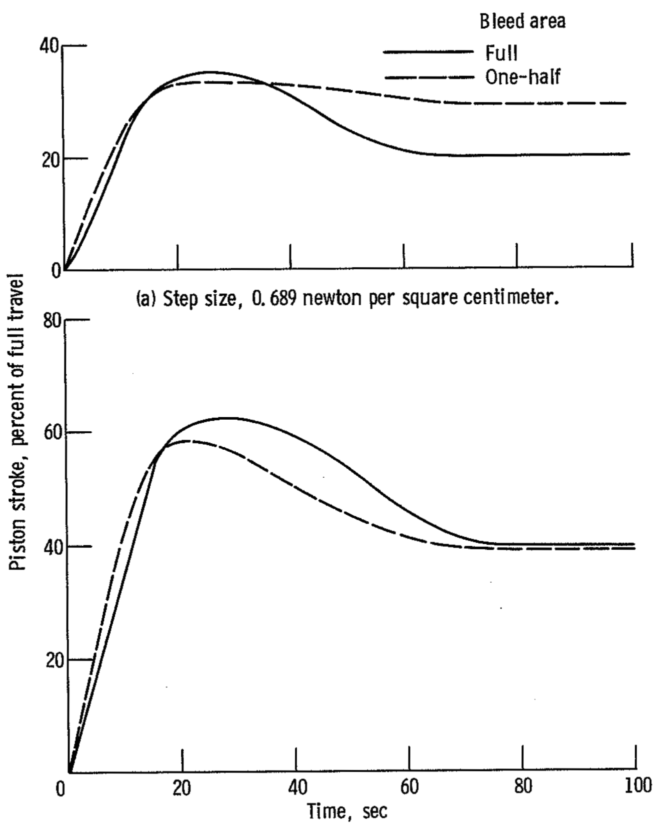

(a) Step size, 0.689 newton per square centimeter.

(b) Step size, 1.034 newtons per square centimeter.

Figure 25. - Effect of size of porous bleed area on response of unshielded relief valve. Initial upstream chamber pressure, 1.59 newtons per square centimeter; spring rate, 8.52 newtons per centimeter; damping orifice diameter, 0.762 centimeter.

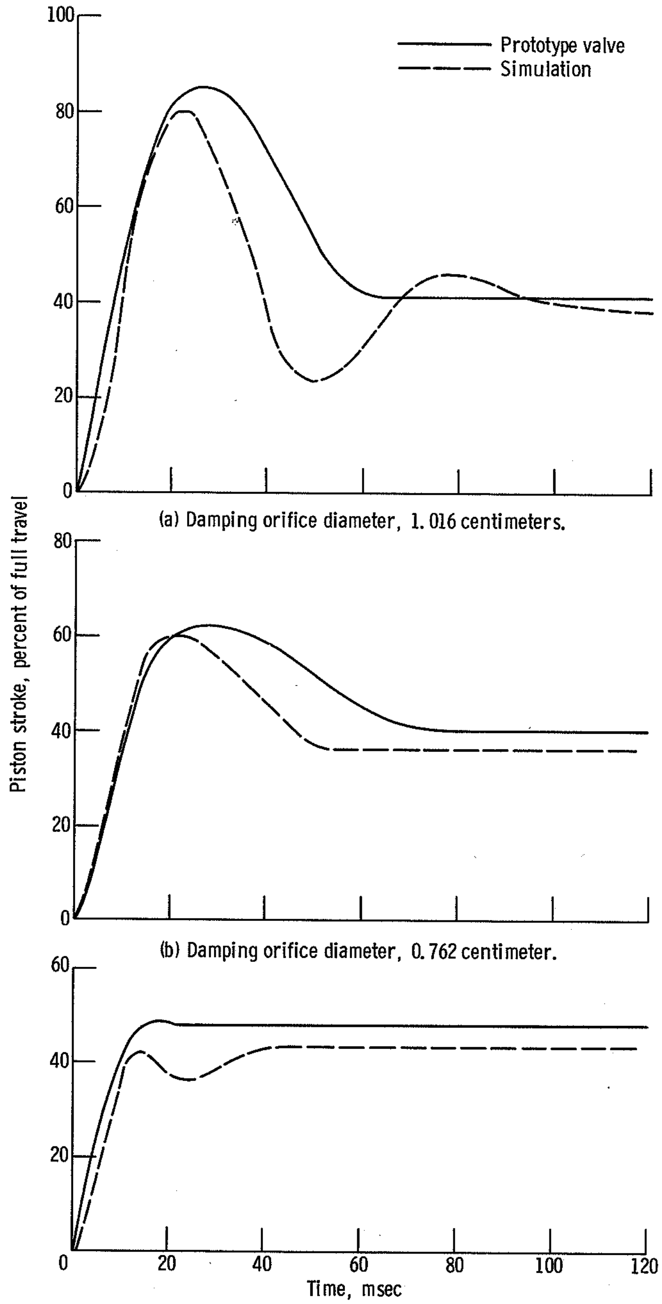

(c) Damping orifice diameter, 0.508 centimeter.

Figure 26. - Comparison of unshielded stability relief valve transient response with simulated valve transient response. Initial upstream chamber pressure, 1.59 newtons per square centimeter; step size, 1.034 newtons per square centimeter.

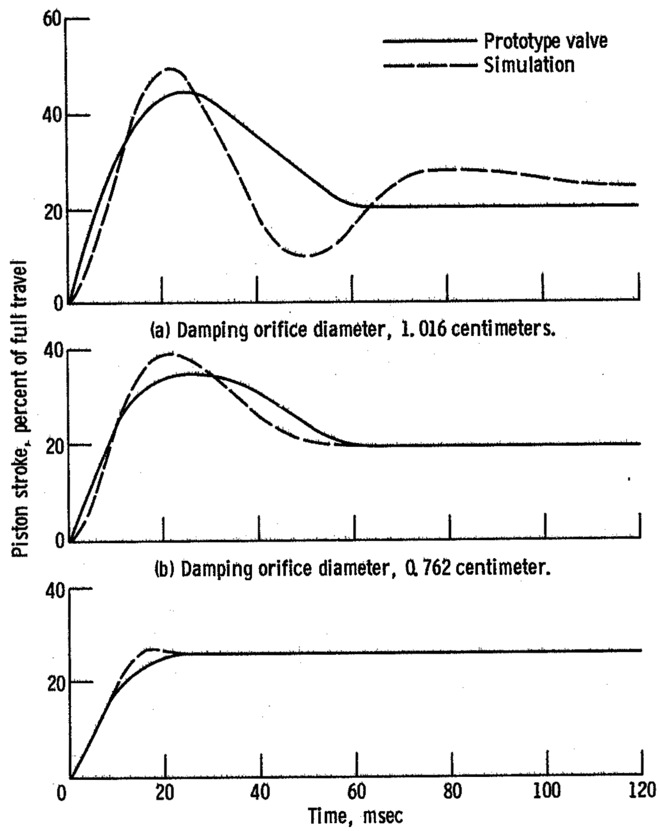

(c) Damping orifice diameter, 0.508 centimeter.

Figure 27. - Comparison of unshielded stability relief valve transient response with simulated valve transient response. Initial upstream chamber pressure, 1.59 newtons per square centimeter; step size, 0.689 newton per square centimeter.

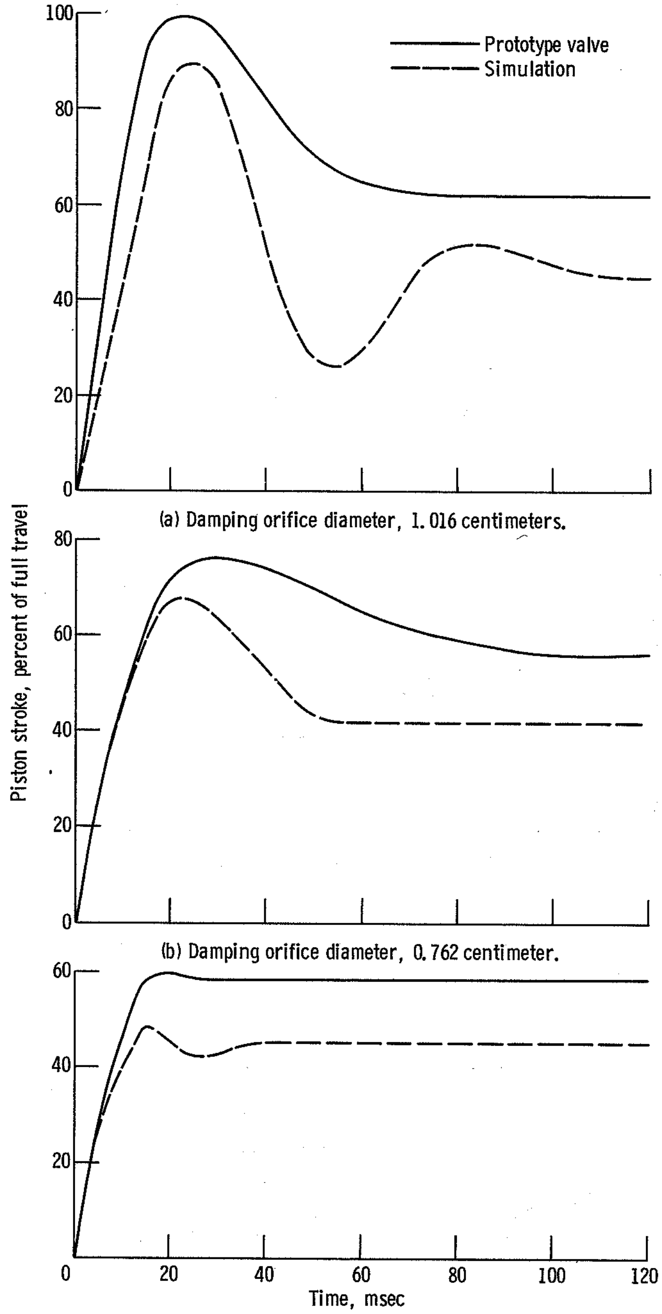

(a) Damping orifice diameter, 1.016 centimeters.

(b) Damping orifice diameter, 0.762 centimeter.

(c) Damping orifice diameter, 0.508 centimeter.

Figure 28. - Comparison of unshielded stability relief valve transient response with simulated valve transient response. Initial upstream chamber pressure, 1.27 newtons per square centimeter; step size, 1.034 newtons per square centimeter.

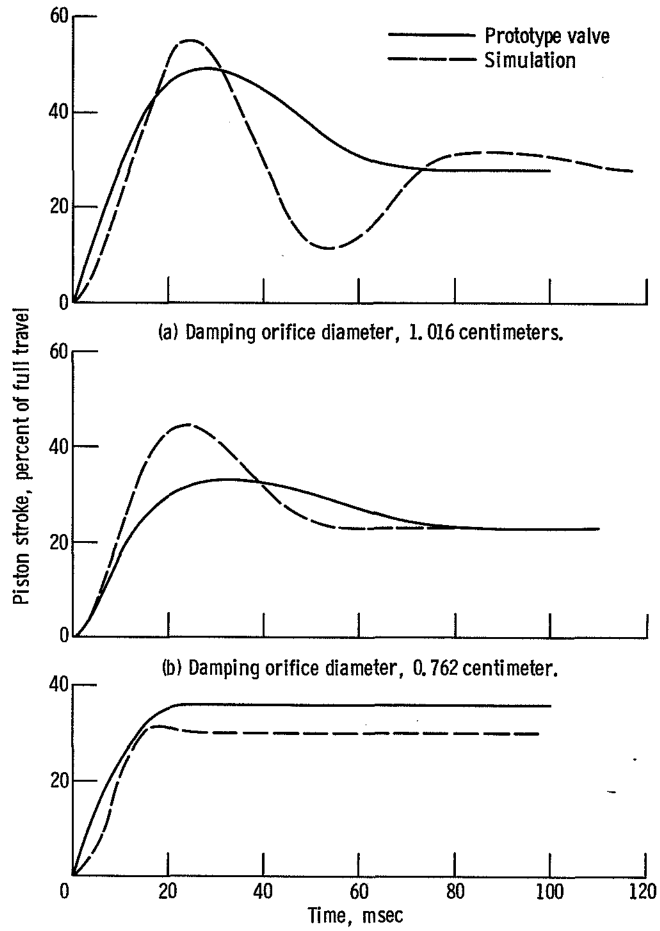

(a) Damping orifice diameter, 1.016 centimeters.

(b) Damping orifice diameter, 0.762 centimeter.

(c) Damping orifice diameter, 0.508 centimeter.

Figure 29. - Comparison of unshielded stability relief valve transient response with simulated valve transient response. Initial upstream chamber pressure, 1.27 newtons per square centimeter; step size, 0.689 newton per square centimeter.

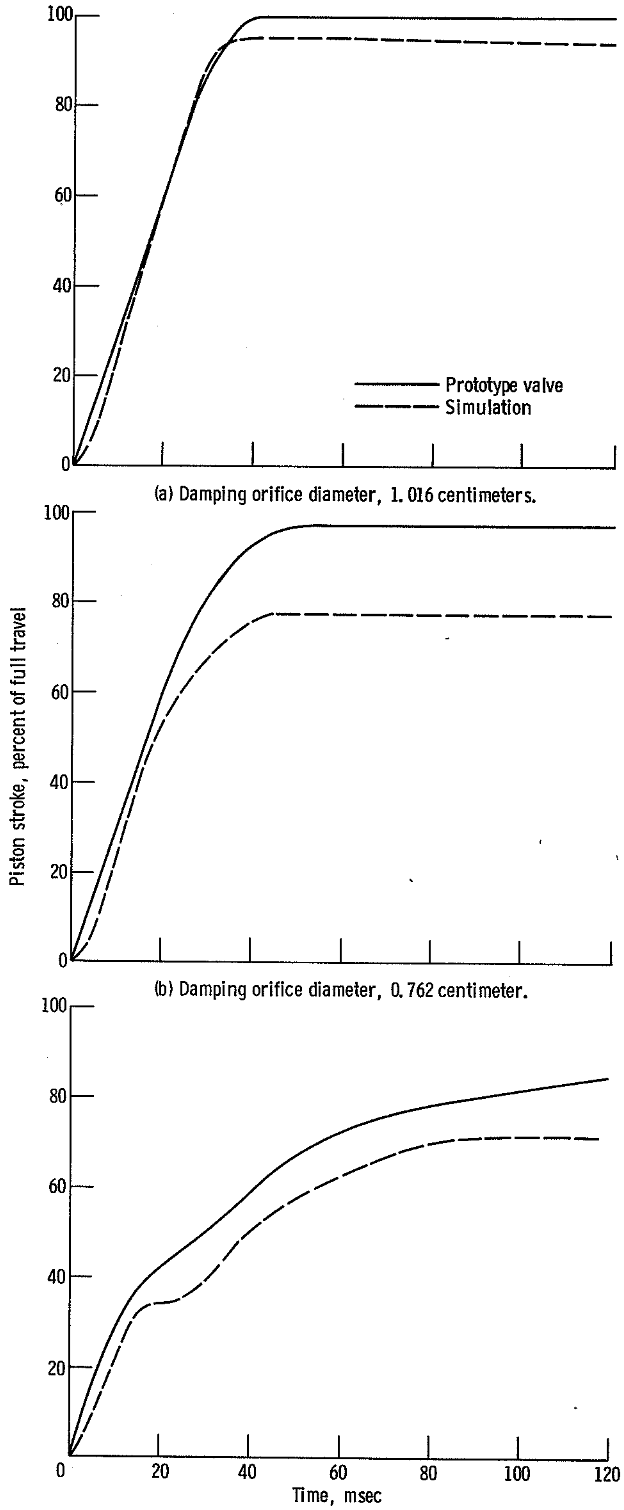

(a) Damping orifice diameter, 1.016 centimeters.

(b) Damping orifice diameter, 0.762 centimeter.

(c) Damping orifice diameter, 0.508 centimeter.

Figure 30. - Comparison of shielded stability relief valve transient response with simulated valve transient response. Initial upstream chamber pressure, 1.59 newtons per square centimeter; step size, 0.758 newton per square centimeter.

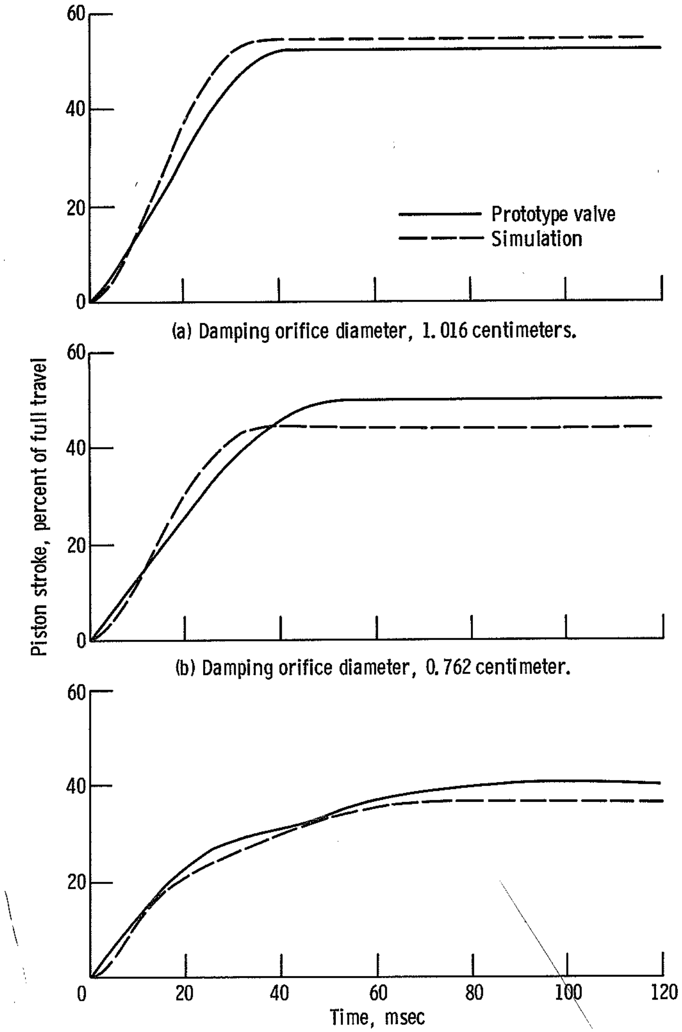

(a) Damping orifice diameter, 1.016 centimeters.

(b) Damping orifice diameter, 0.762 centimeter.

(c) Damping orifice diameter, 0.508 centimeter.

Figure 31. - Comparison of shielded stability relief valve transient response with simulated valve transient response. Initial upstream chamber pressure, 1.59 newtons per square centimeter; step size, 0.552 newton per square centimeter.

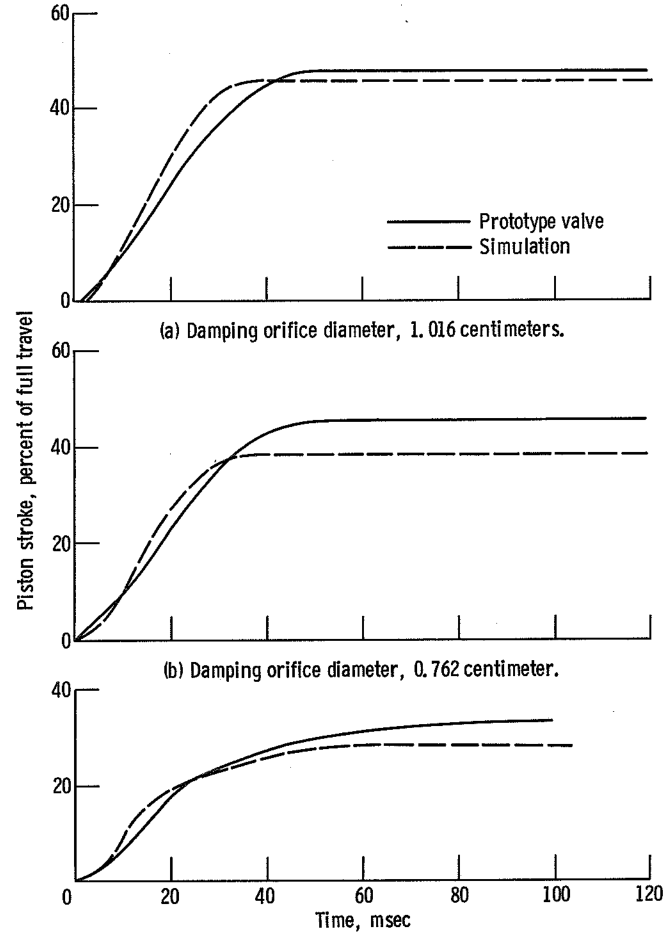

(a) Damping orifice diameter, 1.016 centimeters.

(b) Damping orifice diameter, 0.762 centimeter.

(c) Damping orifice diameter, 0.508 centimeter.

Figure 32. - Comparison of shielded stability relief valve transient response with simulated valve transient response. Initial upstream chamber pressure, 1.27 newtons per square centimeter; step size, 0.483 newton per square centimeter.

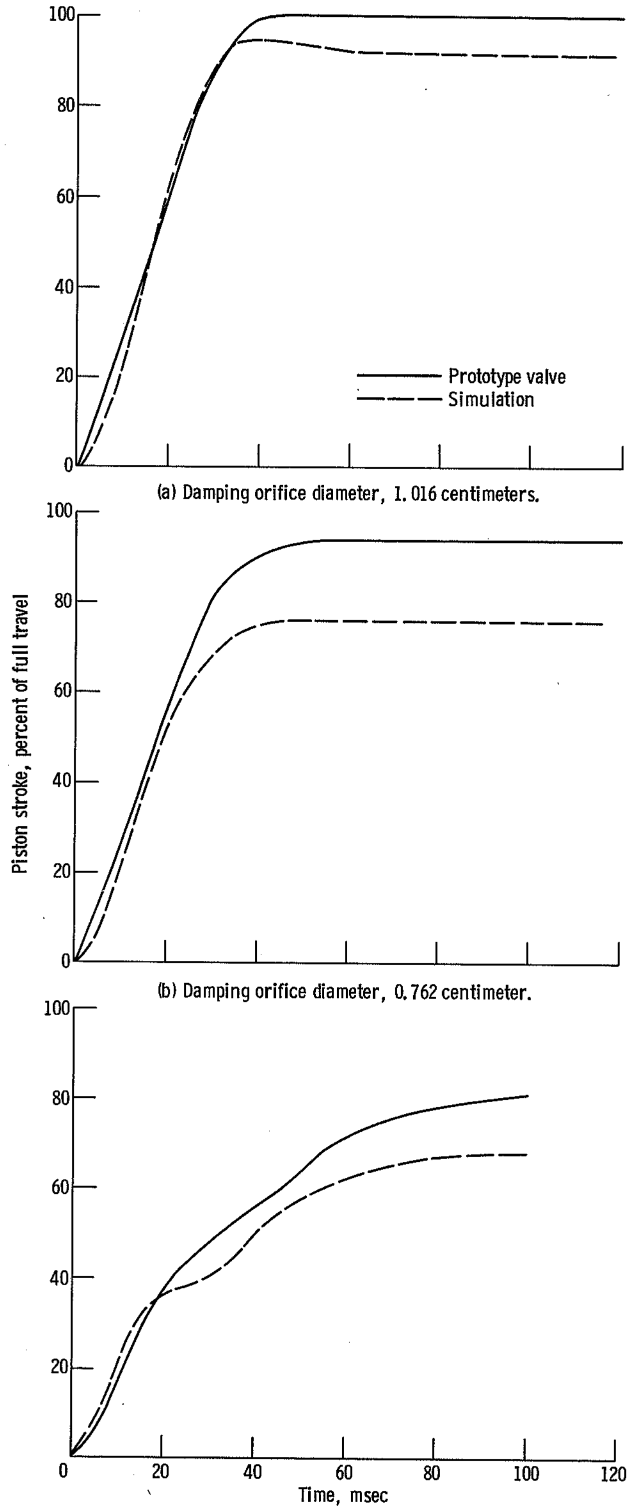

(c) Damping orifice diameter, 0.508 centimeter.

Figure 33. - Comparison of shielded stability relief valve transient response with simulated valve transient response. Initial up-stream chamber pressure, 1.27 newtons per square centimeter; step size, 0.689 newton per square centimeter.

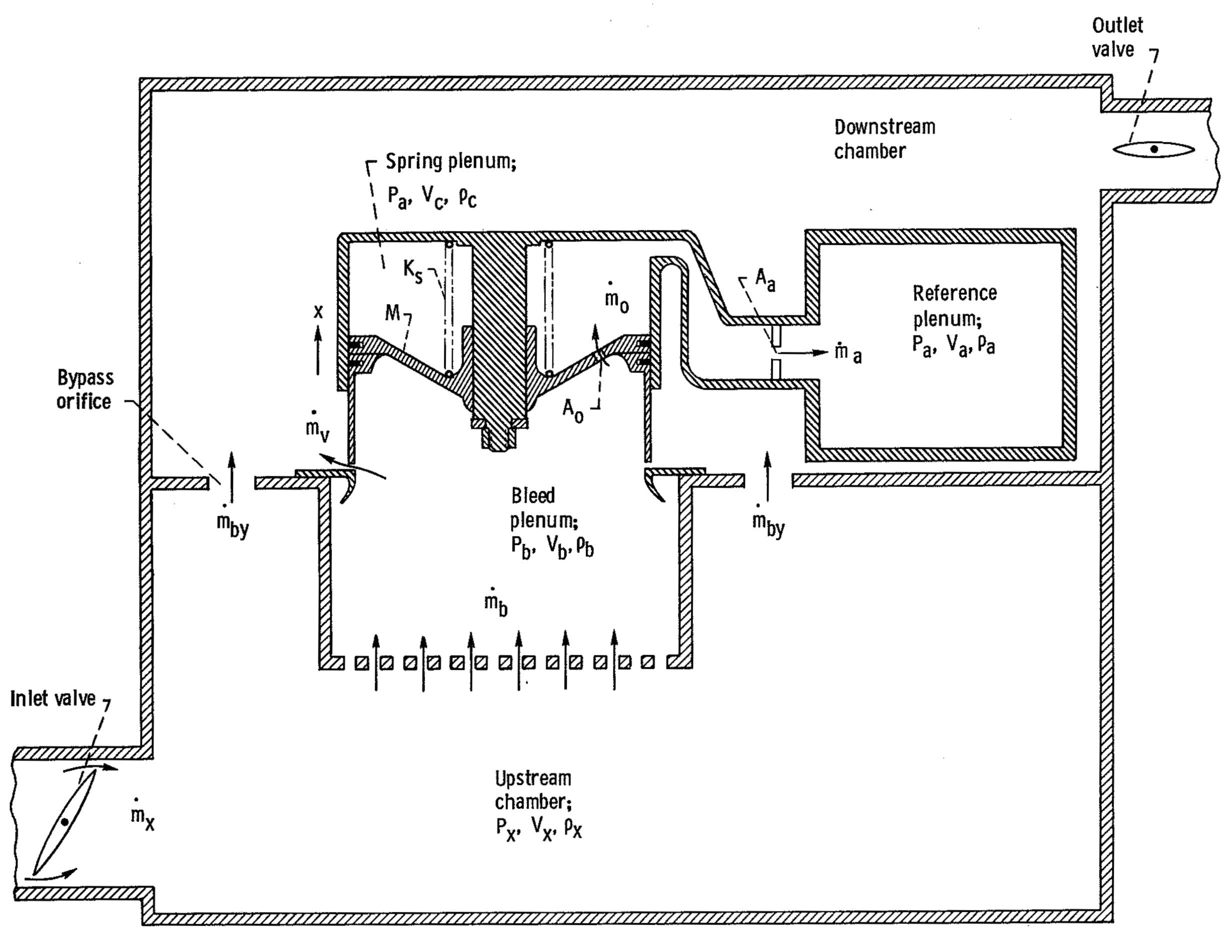

Figure 34. - Simplified schematic of unshielded stability system relief valve for use in analog simulation.

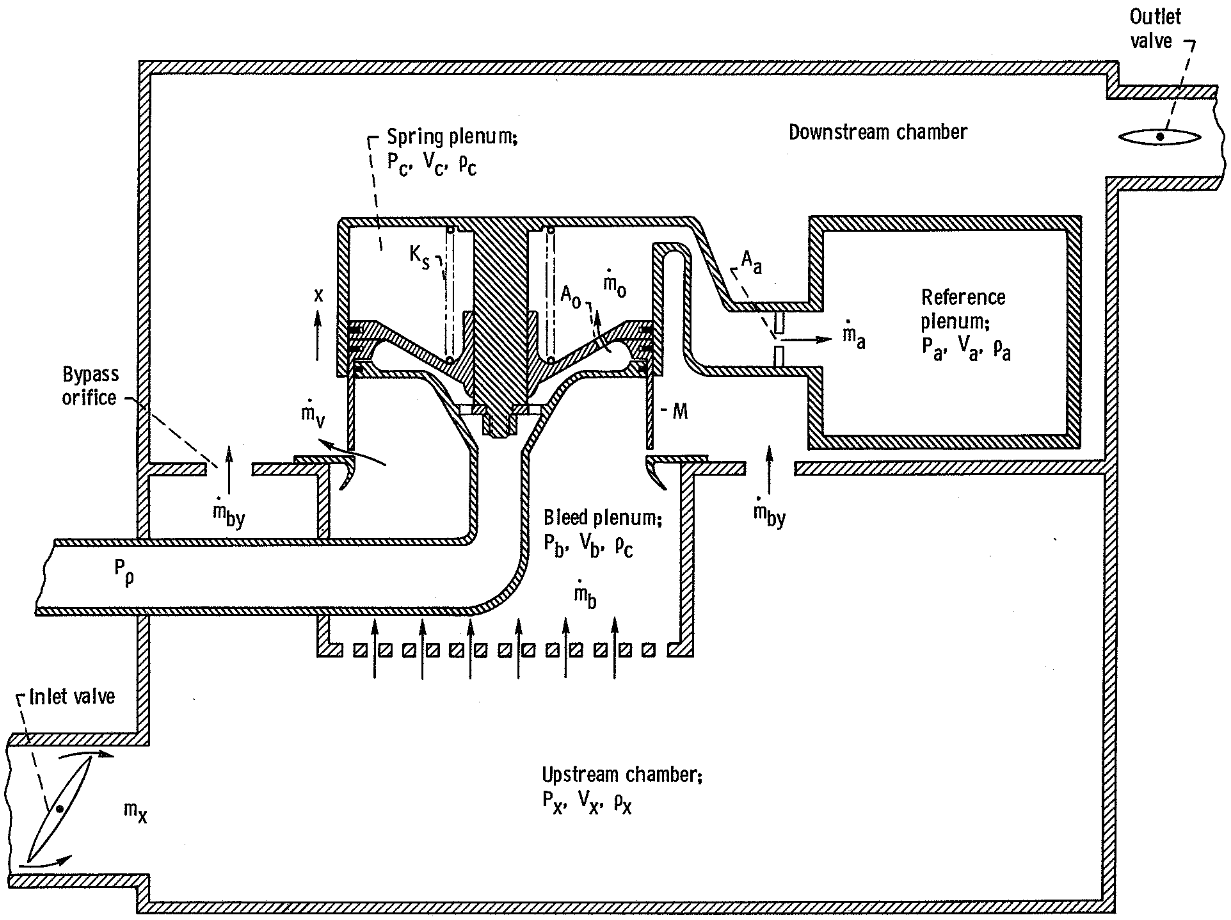

Figure 35. - Simplified schematic of shielded stability system relief valve for use in analog simulation.

"The aeronautical and space activities of the United States shall be conducted so as to contribute . . . to the expansion of human knowledge of phenomena in the atmosphere and space. The Administration shall provide for the widest practicable and appropriate dissemination of information concerning its activities and the results thereof."

—NATIONAL AERONAUTICS AND SPACE ACT OF 1958

NASA SCIENTIFIC AND TECHNICAL PUBLICATIONS

TECHNICAL REPORTS: Scientific and technical information considered important, complete, and a lasting contribution to existing knowledge.

TECHNICAL NOTES: Information less broad in scope but nevertheless of importance as a contribution to existing knowledge.

TECHNICAL MEMORANDUMS: Information receiving limited distribution because of preliminary data, security classification, or other reasons. Also includes conference proceedings with either limited or unlimited distribution.

CONTRACTOR REPORTS: Scientific and technical information generated under a NASA contract or grant and considered an important contribution to existing knowledge.

TECHNICAL TRANSLATIONS: Information published in a foreign language considered to merit NASA distribution in English.

SPECIAL PUBLICATIONS: Information derived from or of value to NASA activities. Publications include final reports of major projects, monographs, data compilations, handbooks, sourcebooks, and special bibliographies.

TECHNOLOGY UTILIZATION PUBLICATIONS: Information on technology used by NASA that may be of particular interest in commercial and other non-aerospace applications. Publications include Tech Briefs, Technology Utilization Reports and Technology Surveys.

Details on the availability of these publications may be obtained from:

SCIENTIFIC AND TECHNICAL INFORMATION OFFICE

NATIONAL AERONAUTICS AND SPACE ADMINISTRATION

Washington, D.C. 20546